[AMERICAN JOURNAL OF SCIENCE, SCHAIRER VOL. 267-A, 1969, P. 509-549]

AN EXPERIMENTAL STUDY ON THE ROLE OF TITANIUM IN ALKALIC BASALTS IN LIGHT OF THE SYSTEM DIOPSIDE-AKERMANITE-NEPHELINE-$CaTiAl_2O_6$

KENZO YAGI and KOSUKE ONUMA
Department of Geology and Mineralogy,
Hokkaido University, Sapporo, Japan

ABSTRACT. Phase equilibria in the six-component system diopside–akermanite–nepheline–$CaTiAl_2O_6$ have been determined at atmospheric pressure. Liquidus and subliquidus results have been obtained on a total of 197 compositions on the bounding planes of the tetrahedron and along four sections parallel to the basal plane, diopside–akermanite–nepheline.

Because of complex solid solutions, the maximum number of coexisting phases in the system is six, and the following four six-phase assemblages are present:

1. forsterite + melilite + nepheline_{ss} + spinel + perovskite + liquid
2. forsterite + melilite + spinel + perovskite + diopside_{ss} + liquid
3. diopside_{ss} + forsterite + melilite + nepheline_{ss} + perovskite + liquid
4. diopside_{ss} + melilite + nepheline_{ss} + perovskite + corundum + liquid

Assemblages 1, 2, and 3 show a reaction relation; each occurs in a small temperature range at various temperatures. Assemblage 4 is eutectic-like. In these critical assemblages the behavior is essentially that of a five-component system. These four assemblages and eight five-phase assemblages are used to construct the courses of crystallization for the pseudo-quinary system.

Crystallization differentiation in this simplified system is applicable to melilite-bearing subsilicic, alkalic magmas. The inferred trend of differentiation is olivine melilitite → olivine melilite nephelinite → perovskite-bearing melilite nephelinite → corundum-bearing melilite nephelinite. Corundum is absent in natural mafic rocks, and it is suggested that it occurs in spinel as a hercynite molecule, in mica, or in amphibole. The titanium in the system occurs mainly in solid solution in the clinopyroxene, which incorporates a maximum of 4 wt percent TiO_2 before perovskite crystallizes.

INTRODUCTION

Titanium is a minor constituent in most basaltic rocks, but its content is high in mafic alkalic rocks, averaging more than 2 percent TiO_2 and being as high as 4 percent TiO_2 in nephelinites or related rocks. Conversely, tholeiitic basalts generally contain less than 2 percent TiO_2. The significance of titanium as a measure of petrographic province was discussed by Chayes (1964) and Chayes and Metais (1964). Chayes mentioned that a discriminant set based on $TiO_2 = 1.75$ percent assigns basalts either to oceanic-island basalts (mostly alkalic) or circumoceanic basalts (mostly tholeiitic).

In the alkalic rocks titanium occurs mainly as sphene, in solid solution in silicates (pyroxene, biotite, or hornblende), as iron-titanium oxides and less commonly as perovskite. Verhoogen (1962) discussed the theoretical aspects of the partitioning of titanium between silicates and oxides and concluded that in strongly undersaturated melts titanium preferentially enters the silicates, the remainder occurring in perovskite and in the iron-titanium oxides. Thus, as a first step toward understanding the behavior of titanium in the alkali basaltic rocks, we have

studied its distribution in the titanium-bearing silicate phases formed at high temperatures.

The most abundant minerals in undersaturated mafic alkalic rocks are olivine, clinopyroxene, plagioclase, nepheline, and melilite. With the exception of plagioclase, these minerals all occur on the liquidus surface in the system diopside–akermanite–nepheline (Onuma and Yagi, 1967). Since the chemistry of the titaniferous pyroxenes in the alkalic rocks shows that substitution of Ti⇌Mg is accompanied by Al⇌Si, a hypothetical "titan pyroxene molecule" $CaTiAl_2O_6$ (abbreviated Tp), which consists of perovskite and corundum at atmospheric pressure, is added to the above named quinary system. The resulting system diopside–akermanite–nepheline–$CaTiAl_2O_6$ encompasses the mineral assemblages that characterize olivine melilite nephelinites, melilite nephelinites, and related alkalic rocks. We have studied the phase equilibria relations in this tetrahedron and present here our initial results on the petrologically more important part of the system. The distribution of titanium between coexisting silicates and oxides will be considered experimentally at a later date.

PREVIOUS WORK

Yoder and Tilley (1962) discussed the simple basalt system of nepheline–diopside–forsterite–silica, which contains both tholeiitic and alkalic basalts. Recently this tetrahedron was expanded to nepheline–forsterite–larnite–silicate to include the strongly undersaturated mafic alkalic rocks containing melilite (Schairer and Yoder, 1964). The system diopside–akermanite–nepheline studied by Onuma and Yagi (1967) is a join in this expanded basalt tetrahedron. This system also serves as the base of the pseudo-quinary system now under consideration.

The titanium-bearing silicate systems have been the subject of a number of studies. DeVries, Roy, and Osborn (1954) studied the system TiO_2–SiO_2 and critically reviewed the inconsistent results obtained by earlier investigators. They also investigated the system CaO–TiO_2–SiO_2 (DeVries, Roy, and Osborn, 1955). Several other titanium-bearing systems such as TiO_2–Al_2O_3–SiO_2 (Agamawi and White, 1952), Na_2O–TiO_2–SiO_2 (Hamilton and Cleek, 1958), and CaO_2–TiO_2–Al_2O_3–SiO_2 (Iwase and Nisioka, 1936; Agamawi and White, 1953, 1954) have been studied, in which phase relations between such minerals as wollastonite, pseudowollastonite, sphene, and anorthite have been discussed. The behavior of titanium in association with FeO or Fe_2O_3 in silicate systems has been studied by MacChesney and Muan (1960) in the system Fe_3O_4–TiO_2–SiO_2 in air and at varying P_{O_2}. These studies contribute primarily to an understanding of the role of titanium from the metallurgical or ceramic rather than the petrogenetic viewpoint. In the present paper emphasis is placed on the mineralogical or petrological aspect of the behavior of titanium in the alkali basaltic rocks, with special reference to equilibria in the silicate systems.

EXPERIMENTAL METHOD

Homogeneous glasses in the system diopside–akermanite–nepheline–$CaTiAl_2O_6$ were prepared by melting pure chemicals in a platinum crucible. Quartz (purified by the method described by Schairer and Bowen, 1955), certified reagents of Al_2O_3, $CaCO_3$, TiO_2, and MgO from Fisher Scientific Company, and pure sodium disilicate (prepared by the same method as described by Schairer and Bowen, 1956) were used. The homogeneity of each glass was verified under the petrographic microscope by its uniformity of refractive index (Schairer, 1959).

The crushed glasses were held at temperatures between 800°C and 1000°C until crystallization of glass was complete. These crystalline mixtures were used as starting material for all the quenching experiments. Phase assemblages of starting materials where determined are listed in table 1.

A platinum wire-wound, electric furnace was used as a quenching furnace, regulated to a precision of ± 1°C. Pt-$Pt_{90}Rh_{10}$ thermocouples used to measure the temperature were calibrated at the standard melting points of NaCl (800.4°C), Au (1062.6°C), and diopside (1391.5°C). Crystalline phases obtained by quenching were identified both by petrographic microscope and X-ray diffractometer.

PHASE DIAGRAMS AND QUENCHING DATA

The system diopside–akermanite–nepheline–$CaTiAl_2O_6$ is pseudo-quaternary, forming part of a six-component system. We have studied the four ternary joins that form the bounding planes of the tetrahedron and four sections parallel to the basal plane, diopside–akermanite–nepheline, with constant $CaTiAl_2O_6$ contents of 5, 10, 15, and 20 wt percent, respectively. The equilibria relations in each of these planes are discussed below. Liquidus and subliquidus determinations have been made on a total of 197 compositions on or within the tetrahedron.

Diopside–akermanite–nepheline.—This join was studied by Schairer and Yoder (1964) and by Onuma and Yagi (1967), and the latter authors' diagram is reproduced here as figure 1. It is pseudo-ternary with two piercing points: (1) E, at 1212°C, has a liquid of composition $Di_{55}Ak_6Ne_{39}$ coexisting with forsterite, $diopside_{ss}$ (ss = solid solution), and melilite; (2) F, at 1169°C, has a liquid of composition $Di_{38}Ak_3Ne_{59}$ coexisting with forsterite, melilite, and $nepheline_{ss}$. Each of these lies on or near univariant lines which meet at 1135° ± 10°C, with a resultant assemblage of forsterite, $diopside_{ss}$, $nepheline_{ss}$, melilite, and liquid. At this point forsterite is consumed to form $diopside_{ss}$ in assemblage (2) and $nepheline_{ss}$ in assemblage (1). Every mixture on this join crystallizes as the phase assemblage $diopside_{ss}$ + $nepheline_{ss}$ + melilite at temperatures below 1135°C ± 10°C, which approximates a reaction point in the system diopside–akermanite–nepheline. The point evolves on addition of the component $CaTiAl_2O_6$ into a point on the six-component surface, $diopside_{ss}$ + forsterite + melilite + $nepheline_{ss}$ + liquid.

TABLE 1

Phase assemblages of selected starting material (crystallized at 1000°C)

Composition, wt %				Time for crystallization, days	Phase assemblage
Di	Ak	Ne	Tp*		
58	30		12	33	Mel + Di + Pv?
54	10		36	15	Mel + Di + Pv?
49	26		25	15	Mel + Di + Pv?
40	10		50	19	Mel + Di + Pv?
20	40		40	17	Mel + Di + Pv?
20	30		50	10	Mel + Di + Pv
10	70		20	11	Mel + Di + Pv? + Sp?
	70	20	10	18	Mel + Ne + Pv
	60	20	20	10	Mel + Ne + Pv
	40	40	20	18	Mel + Ne + Pv + Di?
	40	10	50	30	Mel + Ne + Pv + Di + Cor?
	35	25	40	16	Mel + Ne + Pv + Di? + Cor
	33	56	11	16	Mel + Ne + Pv + Di? + Cor?
	30	20	50	25	Mel + Ne + Pv + Di? + Cor
	20	65	15	30	Mel + Ne + Pv
	20	60	20	30	Mel + Ne + Pv
	10	70	20	30	Ne + Pv + Cor?
80		10	10	28	Di + Ne + Mel + Pv
65		2	33	15	Di + Ne + Mel + Pv
60		10	30	14	Di + Ne + Mel
57		10	33	10	Di + Ne + Mel + Pv?
40		50	10	14	Di? + Ne + Mel + Cor + Pv
40		30	30	21	Di + Ne + Mel + Pv + Cor?
10		80	10	25	Di? + Ne + Mel + Pv + Cor
72	10	13	5	7	Di + Mel + Ne
65	20	10	5	22	Di + Mel + Ne + Pv + Cor
55	20	20	5	38	Di + Mel + Ne + Pv?
68	20	2	10	18	Di + Mel + Ne
67	21	2	10	7	Di + Mel + Ne + Pv? + Cor?
50	10	30	10	14	Di + Mel + Ne + Pv + Cor
40	4	46	10	48	Di? + Mel + Ne + Pv + Cor
39	5	46	10	30	Di? + Mel + Ne + Pv + Cor
6	27	57	10	18	Di + Mel + Ne + Pv + Cor
64	20	1	15	51	Mel + Di + Pv?
46	5	34	15	34	Mel + Di + Ne + Pv + Cor
54	6	20	20	11	Di + Mel + Ne + Pv + Cor?
53	6	21	20	14	Di + Mel + Ne + Pv + Cor?
40	23	17	20	40	Di + Mel + Ne + Pv + Cor?
40	10	30	20	6	Di + Mel + Ne + Pv + Cor

*$CaTiAl_2O_6$.

Abbreviations for this and subsequent tables: Ak, akermanite; Cor, corundum; Di, diopside; Fo, forsterite; Mel, melilite; Ne, nepheline; Cg, carnegieite; Pv, perovskite; Sp, spinel; h, hours; d, days.

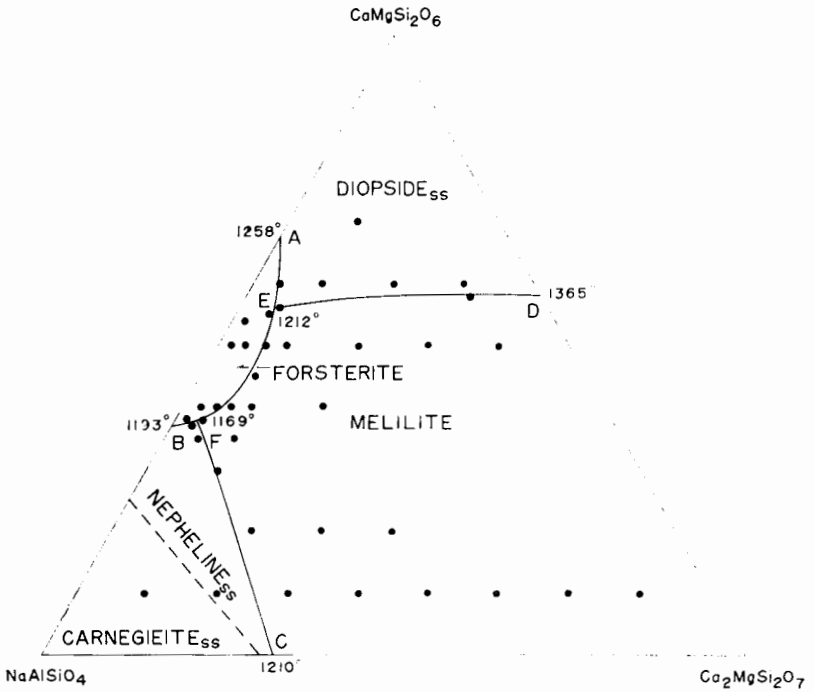

Fig. 1. Liquidus diagram for the join diopside–akermanite–nepheline (Onuma and Yagi, 1967). Dots indicate compositions studied.

Diopside–akermanite–$CaTiAl_2O_6$.—Yagi and Onuma (1967) investigated one of the limiting systems of this join, diopside–$CaTiAl_2O_6$, and found it to be pseudo-binary. Diopside, which incorporates up to 11 wt percent $CaTiAl_2O_6$ molecule, akermanite, perovskite, forsterite, and spinel are the crystalline phases (fig. 2). No evidence was found for the formation of garnet at temperatures of 1000°C and higher, although garnet solid solution is present in the analogous system $CaMgSi_2O_6$–$CaTiFe_2O_6$ (Huckenholz, 1969). Presumably this garnet solid solution is andraditic in composition, whereas if garnet does form in the present system, it should be grossularitic. From Yoder's (1950) experiments it appears that such garnet can form at atmospheric pressure below about 750°C at an exceptionally slow rate. Appearance of forsterite as a primary phase and its subsequent reaction with liquid until consumed are worthy of note.

The join diopside–akermanite–$CaTiAl_2O_6$ is shown in figure 3, and the quenching data are summarized in table 2. Three crystalline phases coexist with liquid at two points (K and L of fig. 3). Both K ($Di_{48}Ak_{26}Tp_{26}$) and L ($Di_{58}Ak_{25}Tp_{17}$) are piercing points in the system diopside–akermanite–perovskite–spinel. The two univariant lines, forsterite + akermanite + perovskite + liquid (K) and forsterite + diopside$_{ss}$ + akermanite + liquid (L), form an invariant point at about

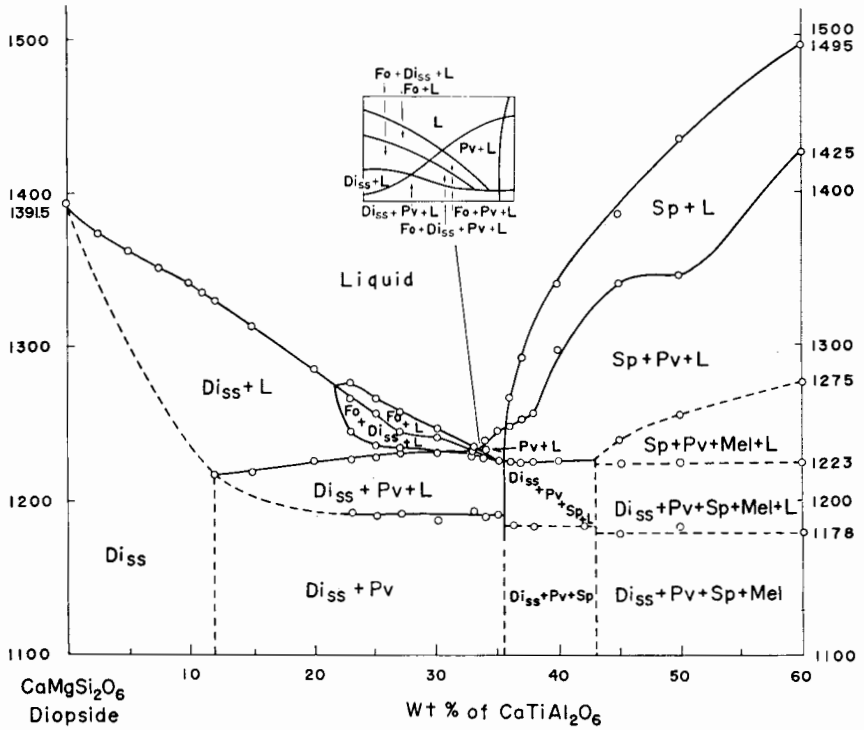

Fig. 2. Pseudobinary diagram of the join diopside–$CaTiAl_2O_6$ (Yagi and Onuma, 1967). Di_{ss} = diopside solid solution, Fo = forsterite, L = liquid, Mel = melilite, Pv = perovskite, Sp = spinel.

1230°C, the temperature at which forsterite reacts with liquid. Upon lowering of temperature the assemblage $diopside_{ss}$ + akermanite + perovskite + liquid continues to crystallize until the eutectic point is attained where spinel appears.

Diopside–nepheline–$CaTiAl_2O_6$.—Figure 4 shows the primary fields for this join, and the quenching data are listed in table 3. There are four points at which three crystalline phases coexist with liquid (M, N, O, and P of fig. 4).

Melilite appears as the third or fourth phase in every mixture even though it does not have its own primary field on the liquidus surface. Forsterite and spinel react with liquid at low temperatures and disappear.

A five-phase assemblage was found for the composition $Di_{40}Ne_{30}Tp_{30}$ where spinel, forsterite, $nepheline_{ss}$, and perovskite coexist with liquid. Another five-phase assemblage is suggested in the vicinity of point O with the addition of melilite to the assemblage forsterite + $nepheline_{ss}$ + spinel + liquid.

The phase assemblages of the starting materials in this system indicate that the subsolidus phase assemblage near the join diopside–

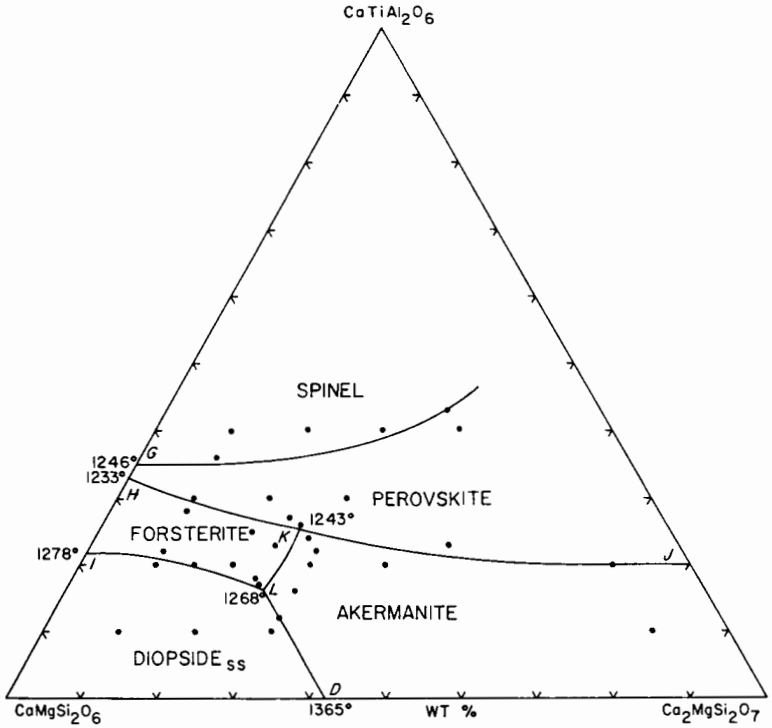

Fig. 3. Liquidus diagram for the join diopside–akermanite–$CaTiAl_2O_6$.

$CaTiAl_2O_6$ is $diopside_{ss}$ + melilite + $nepheline_{ss}$ + perovskite. The final phase assemblage for mixtures around O, N, and M is $diopside_{ss}$ + melilite + $nepheline_{ss}$ + perovskite + corundum; the solidus temperature is about 1105°C.

Nepheline–akermanite–$CaTiAl_2O_6$.—The phase diagram for this join is shown in figure 5, and the quenching data are listed in table 4. Points Q, R, S, and T represent four-phase assemblages (three solid phases and liquid).

Forsterite and $diopside_{ss}$ appear as third or fourth phases, but they do not appear on the liquidus. Three five-phase assemblages are present: near point T, forsterite joins the assemblage melilite + perovskite + spinel + liquid as the fourth crystalline phase; and near point S, perovskite joins the assemblage $nepheline_{ss}$ + spinel + melilite + liquid for some compositions, and forsterite joins the assemblage melilite + $nepheline_{ss}$ + spinel + liquid for other compositions. The first two of these assemblages demonstrably continue crystallization toward a six-phase assemblage (1, fig. 11). Crystallization at and beyond this point is discussed subsequently.

TABLE 2

The join diopside-akermanite-$CaTiAl_2O_6$

Composition, wt %			Temp, °C	Time	Phases
Di	Ak	Tp			
80	10	10	1335	15 h	Glass
			1330	2 h	Trace Di + glass
			1225	72 h	Di + glass
			1220	72 h	Di + Pv + glass
70	20	10	1325	2 h	Glass
			1320	15 h	Trace Di + glass
			1255	2 h	Di + glass
			1250	3 h	Di + Ak + glass
			1230	72 h	Di + Ak + glass
			1225	96 h	Di + Ak + Pv + glass
60	30	10	1310	2 h	Glass
			1305	2 h	Di + trace Ak + glass
			1235	72 h	Di + Ak + glass
			1230	72 h	Di + Ak + trace Pv + glass
10	80	10	1390	2 h	Glass
			1385	2 h	Ak + glass
			1290	2 h	Ak + glass
			1285	3 h	Ak + trace Pv + glass
58	30	12	1305	20 h	Glass
			1300	2 h	Ak + trace Di + glass
			1285	2 h	Ak + Di + glass
			1280	2 h	Ak + Di + trace Fo + glass
			1275	2 h	Ak + Di + trace Fo + glass
			1270	2 h	Ak + Di + glass
			1240	24 h	Ak + Di + glass
54	30	16	1290	2 h	Glass
			1285	2 h	Trace Ak + glass
			1275	2 h	Ak + glass
			1270	2 h	Ak + Fo + glass
			1265	2 h	Ak + Fo + Di + glass
			1240	15 h	Ak + trace Fo + Di + glass
			1235	15 h	Ak + Di + glass
			1230	15 h	Ak + Di + Pv + glass
58	25	17	1275	2 h	Glass
			1270	3 h	Trace Fo + glass
			1265	20 h	Fo + Di + Ak + glass
			1245	20 h	Fo + Di + Ak + glass
			1240	24 h	Di + Ak + glass
			1235	72 h	Di + Ak + glass
			1230	72 h	Di + Ak + Pv + glass
58	24	18	1275	2 h	Glass
			1270	2 h	Trace Fo + glass
			1265	20 h	Fo + Di + Ak + glass
			1240	72 h	Trace Fo + Di + Ak + glass
			1235	24 h	Di + Ak + glass
			1230	72 h	Di + Ak + Pv + glass

TABLE 2 (continued)

Composition, wt %			Temp, °C	Time	Phases
Di	Ak	Tp			
70	10	20	1275	2 h	Glass
			1270	2 h	Di + glass
			1230	48 h	Di + Ak + glass
			1225	72 h	Di + Ak + glass
65	15	20	1275	2 h	Glass
			1270	20 h	Fo + glass
			1265	20 h	Fo + Di + glass
			1235	72 h	Trace Fo + Di + glass
			1230	72 h	Di + Pv + glass
60	20	20	1265	2 h	Glass
			1260	2 h	Trace Fo + glass
			1250	15 h	Fo + glass
			1245	15 h	Fo + Di + glass
			1240	15 h	Di + glass
			1235	72 h	Di + glass
			1230	20 h	Di + Pv + glass
50	30	20	1280	2 h	Glass
			1275	2 h	Trace Ak + glass
			1265	20 h	Ak + glass
			1260	2 h	Ak + Fo + glass
			1245	15 h	Ak + Fo + glass
			1240	15 h	Ak + Di + glass
			1230	48 h	Ak + Di + glass
			1225	72 h	Ak + Di + Pv + glass
40	40	20	1295	2 h	Glass
			1290	15 h	Ak + glass
			1250	20 h	Ak + glass
			1245	3 h	Ak + trace Fo + glass
			1240	20 h	Ak + Fo + glass
			1235	72 h	Ak + Fo + trace Pv + glass
			1230	48 h	Ak + trace Fo + Pv + glass
			1225	72 h	Ak + Pv + Di + glass
10	70	20	1340	2 h	Glass
			1335	2 h	Ak + trace Pv + glass
68	10	22	1270	2 h	Glass
			1265	20 h	Trace Fo + glass
			1260	20 h	Fo + Di + glass
			1240	24 h	Trace Fo + Di + glass
			1235	72 h	Di + glass
			1230	72 h	Di + Pv + glass
48	30	22	1270	2 h	Glass
			1265	2 h	Ak + glass
			1260	2 h	Ak + glass
			1255	2 h	Ak + Fo + glass
			1235	15 h	Ak + Fo + glass
			1230	15 h	Ak + Fo + Di + Pv + glass
			1225	72 h	Ak + trace Fo + Di + Pv + glass
			1220	72 h	Ak + Di + Pv + glass

TABLE 2 (continued)

Composition, wt %			Temp, °C	Time	Phases
Di	Ak	Tp			
53	24	23	1260	2 h	Glass
			1255	2 h	Trace Fo + glass
			1240	5 h	Fo + Ak + glass
			1235	20 h	Fo + Ak + Di + glass
			1230	20 h	Ak + Di + Pv + glass
30	47	23	1330	2 h	Glass
			1325	2 h	Pv + glass
			1320	2 h	Pv + glass
			1315	20 h	Pv + Ak + glass
			1305	2 h	Pv + Ak + glass
			1300	2 h	Pv + Ak + trace Fo + glass
			1230	72 h	Pv + Ak + Fo + glass
			1220	72 h	Pv + Ak + Di + glass
48	28	24	1260	2 h	Glass
			1255	2 h	Trace Ak + glass
			1250	2 h	Ak + trace Fo + glass
			1240	15 h	Ak + Fo + glass
			1235	24 h	Ak + Fo + trace Pv + glass
			1230	20 h	Ak + Fo + Pv + glass
			1225	72 h	Ak + Pv + Di + glass
55	20	25	1260	2 h	Glass
			1255	24 h	Trace Fo + glass
			1240	72 h	Fo + glass
			1235	72 h	Fo + Di + glass
			1230	72 h	Di + Pv + glass
49	26	25	1250	2 h	Glass
			1245	20 h	Trace Fo + trace Ak + glass
			1240	24 h	Fo + Ak + trace Pv + glass
			1235	72 h	Fo + Ak + Pv + glass
			1230	72 h	Fo + Ak + Pv + glass
			1225	72 h	Ak + Pv + Di + glass
48	26	26	1245	24 h	Glass
			1240	2 h	Pv + Fo + Ak + glass
			1230	22 h	Pv + Fo + Ak + glass
			1225	72 h	Pv + Ak + Di + glass
49	24	27	1255	2 h	Glass
			1250	20 h	Pv + Fo + glass
			1235	24 h	Pv + Fo + glass
			1230	20 h	Pv + Fo + Ak + glass
			1225	72 h	Pv + Fo + Ak + Di + glass
			1220	72 h	Pv + Ak + Di + glass
62	10	28	1270	2 h	Glass
			1265	2 h	Trace Fo + glass
			1260	20 h	Fo + glass
			1255	24 h	Fo + Pv + glass
			1235	24 h	Fo + Pv + glass
			1230	72 h	Fo + Pv + trace Di + glass
			1225	72 h	Fo + Pv + Di + glass
			1220	72 h	Pv + Di + glass

TABLE 2 (continued)

Composition, wt %			Temp, °C	Time	Phases
Di	Ak	Tp			
60	10	30	1245	20 h	Glass
			1240	20 h	Trace Pv + glass
			1230	48 h	Pv + glass
			1225	72 h	Pv + Di + glass
50	20	30	1260	2 h	Glass
			1255	2 h	Pv + glass
			1240	15 h	Pv + glass
			1235	72 h	Pv + Di + glass
40	30	30	1310	13 h	Glass
			1305	2 h	Pv + glass
			1235	20 h	Pv + glass
			1230	20 h	Pv + trace Fo + glass
			1225	72 h	Pv + trace Fo + Di + Ak + glass
			1220	72 h	Pv + Di + Ak + glass
54	10	36	1305	18 h	Glass
			1300	2 h	Trace Sp + glass
			1285	3 h	Sp + glass
			1280	2 h	Sp + Pv + glass
			1240	20 h	Sp + Pv + glass
			1235	72 h	Sp + Pv + trace Di + glass
			1230	72 h	Sp + Pv + Di + glass
50	10	40	1350	2 h	Glass
			1345	2 h	Sp + glass
			1335	15 h	Sp + glass
			1330	48 h	Sp + Pv + glass
			1225	72 h	Sp + Pv + Di + glass
			1210	7 d	Sp + Pv + Di + Ak?
40	20	40	1370	2 h	Glass
			1365	2 h	Sp + glass
			1350	3 h	Sp + glass
			1345	2 h	Sp + Pv + glass
			1230	120 h	Sp + Pv + glass
			1225	96 h	Sp + Pv + Di + Ak
30	30	40	1390	2 h	Glass
			1385	2 h	Sp + glass
			1380	3 h	Sp + glass
			1375	2 h	Sp + Pv + glass
			1230	120 h	Sp + Pv + glass
			1225	72 h	Sp + Pv + Ak? + glass
			1220	72 h	Sp + Pv + Ak? + Di
20	40	40	1415	1 h	Glass
			1410	1 h	Trace Pv + glass
20	37	43	1420	1 h	Glass
			1415	1 h	Pv + Sp + glass

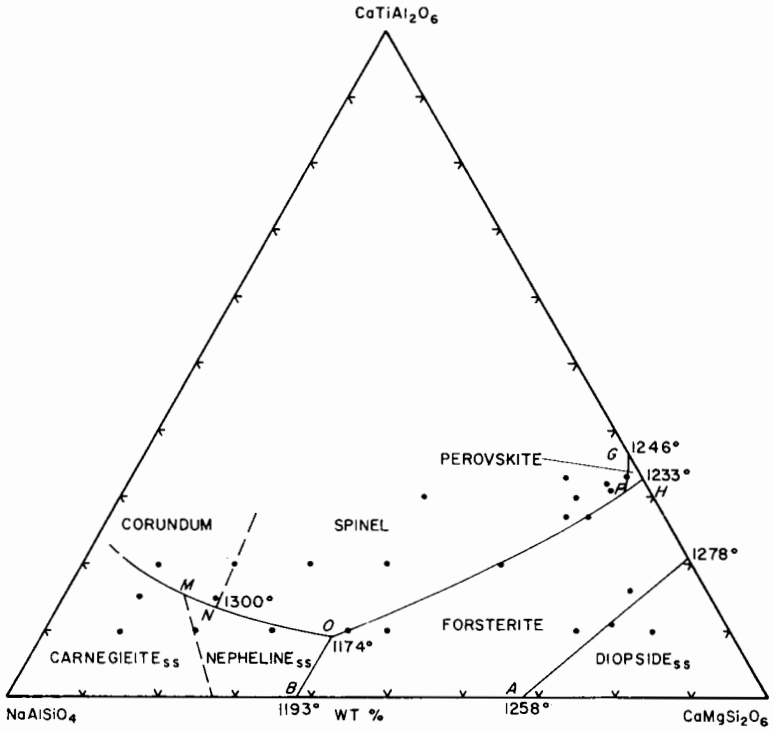

Fig. 4. Liquidus diagram for the join diopside–nepheline–$CaTiAl_2O_6$.

The starting phase assemblage for some of the compositions in the spinel and perovskite fields is $diopside_{ss}$ + $nepheline_{ss}$ + perovskite + melilite + corundum. The corundum occurs in liquidus runs and in most of the starting mixtures which were crystallized at 1000°C for 14 to 30 days (table 1) except for those in the vicinity of point T, perhaps because of the small amount of Al_2O_3 in these compositions. The presence of corundum is indicated optically and by an X-ray reflection at 2.085 Å, corresponding to the (113) spacing. The corundum is regarded as being stable in the system.

Sections parallel to diopside–akermanite–nepheline.—The phase diagrams showing the addition of 5 percent, 10 percent, 15 percent, and 20 percent $CaTiAl_2O_6$ to the join diopside–nepheline–akermanite are shown in figures 6 to 9, and the corresponding quenching data are given in tables 5 to 8, respectively.

The 5 percent plane (fig. 6) has two points (E_1 and F_1) at which three crystalline phases coexist with liquid. This plane is similar to the join diopside–akermanite–nepheline in that it contains one five-phase assemblage, melilite + forsterite + $diopside_{ss}$ + $nepheline_{ss}$ + liquid at 1135° to 1140°C. Forsterite is consumed in this interval, and the resulting

TABLE 3

The join diopside-nepheline-$CaTiAl_2O_6$

Composition, wt %			Temp, °C	Time	Phases
Di	Ne	Tp			
80	10	10	1280	3 h	Trace Di + glass
			1260	18 h	Di + glass
			1255	3 h	Di + trace Fo + glass
			1190	48 h	Di + trace Fo + glass
			1185	48 h	Di + Mel + glass
70	20	10	1260	3 h	Glass
			1255	2 h	Fo + glass
			1250	3 h	Fo + trace Di + glass
			1190	72 h	Fo + Di + trace Mel + glass
			1110	7 d	Barely fritted cake (Di + Mel + Pv)
			1100	7 d	Loose powder (Di + Mel + Pv)
45	45	10	1200	18 h	Trace Fo + glass
			1160	72 h	Fo + glass
			1155	72 h	Fo + Mel + glass
			1150	72 h	Fo + Mel + Ne + Sp? + glass
			1110	7 d	Barely fritted cake (Di + Mel + Ne + Pv?)
			1100	7 d	Loose powder (Di + Mel + Ne + Pv?)
40	50	10	1180	3 h	Glass
			1175	48 h	Fo + trace Sp + glass
			1170	18 h	Fo + Sp? + Ne + glass
			1110	7 d	Fritted cake
			1100	7 d	Loose powder
30	60	10	1225	3 h	Glass
			1220	3 h	Ne + glass
			1215	20 h	Ne + Sp + Cor? + glass
			1165	72 h	Ne + Sp + Cor? + glass
			1160	96 h	Ne + Sp + Cor + Fo + glass*
20	70	10	1275	3 h	Glass
			1270	3 h	Ne + glass
			1265	4 h	Ne + Cor + glass
			1255	24 h	Ne + Cor + glass
			1250	18 h	Ne + Cor + trace Sp + glass
			1160	96 h	Ne + Cor + Sp + trace Fo + trace Pv + glass*
10	80	10	1340	3 h	Glass
			1335	3 h	Cg + glass
			1280	33 h	Cg + glass
			1275	33 h	Cg + trace Ne + glass
			1260	3 h	Cg + Ne + glass
			1255	3 h	Cg + Ne + trace Sp + glass
			1250	72 h	Ne + Sp + glass
			1190	72 h	Ne + Sp + glass
			1180	72 h	Ne + Sp + trace Fo + glass
74	15	11	1265	3 h	Glass
			1260	18 h	Di + trace Fo + glass
			1190	48 h	Di + Fo + glass
			1180	72 h	Di + Fo + Mel + glass

TABLE 3 (continued)

Composition, wt %			Temp, °C	Time	Phases
Di	Ne	Tp			
20	65	15	1320	3 h	Glass
			1315	2 h	Trace Cor + glass
			1305	20 h	Cor + Sp + glass
			1255	3 h	Cor + Sp + glass
			1250	3 h	Cor + Sp + Ne + glass
10	75	15	1315	4 h	Trace Cg + glass
			1305	4 h	Cg + glass
			1300	18 h	Cg + Cor + glass
74	10	16	1275	2 h	Glass
			1270	2 h	Trace Fo + glass
			1260	2 h	Fo + glass
			1255	2 h	Fo + Di + glass
			1200	72 h	Fo + Di + glass
			1190	72 h	Fo + Di + trace Mel + glass
			1175	96 h	Trace Fo + Di + Mel + glass
			1170	72 h	Di + Mel + glass
			1110	7 d	Barely fritted cake (Di + Mel + Pv?)
			1100	7 d	Loose powder (Di + Mel + Pv?)
55	25	20	1220	2 h	Glass
			1215	2 h	Fo + glass
			1185	24 h	Fo + glass
			1180	24 h	Fo + Di + glass
			1150	96 h	Fo + Di + trace Pv + glass
			1140	96 h	Di + Pv + Mel? + glass
40	40	20	1265	3 h	Glass
			1260	18 h	Sp + glass
			1200	48 h	Sp + glass
			1195	72 h	Sp + trace Pv + glass
			1150	96 h	Sp + Pv + glass
30	50	20	1320	72 h	Glass
			1315	24 h	Sp + glass
			1210	18 h	Sp + trace Pv? + glass
			1200	18 h	Sp + Pv? + Ne + glass
20	60	20	1335	2 h	Glass
			1330	18 h	Cor + Sp? + glass
			1235	72 h	Cor + Sp? + glass
			1230	24 h	Cor + Sp + Ne + glass
10	70	20	1320	2 h	Glass
			1315	3 h	Cor + glass
			1310	3 h	Cor + Cg + glass
63	10	27	1235	2 h	Glass
			1230	3 h	Trace Fo + glass
			1220	2 h	Fo + glass
			1215	2 h	Fo + trace Di + glass
			1210	3 h	Fo + Di + glass
			1205	3 h	Fo + Di + trace Pv + glass
			1130	7 d	Loose powder (Di + Mel + Pv)

TABLE 3 (continued)

Composition, wt %			Temp, °C	Time	Phases
Di	Ne	Tp			
60	13	27	1260	3 h	Glass
			1255	3 h	Sp + glass
			1205	72 h	Sp + glass
			1200	3 h	Di + Pv + glass
60	10	30	1245	18 h	Glass
			1240	18 h	Sp + glass
			1225	18 h	Sp + glass
			1220	2 h	Sp + Pv + glass
			1215	24 h	Sp + Pv + Fo + glass
			1210	24 h	Pv + trace Fo + Di + glass
			1200	48 h	Pv + trace Fo + Di + glass
			1195	72 h	Pv + Di + glass
40	30	30	1340	3 h	Glass
			1335	3 h	Sp + glass
			1235	72 h	Sp + glass
			1230	24 h	Sp + Pv + glass
			1170	72 h	Sp + Pv + glass
			1160	72 h	Sp + Pv + Fo? + glass
			1155	96 h	Sp + Pv + Fo + Ne + glass
64	5	31	1235	3 h	Glass
			1230	2 h	Trace Sp + glass
			1228	3 h	Sp + Fo + glass
			1227	3 h	Trace Sp + Fo + Di + glass
			1225	18 h	Trace Sp + Fo + Di + trace Pv + glass
			1220	2 h	Trace Fo + Di + Pv + glass
65	2	33	1250	3 h	Glass
			1245	3 h	Sp + glass
			1235	3 h	Sp + glass
			1233	3 h	Sp + trace Pv + glass
			1230	18 h	Pv + Di + glass
63	5	32	1240	18 h	Glass
			1235	15 h	Sp + glass
			1230	3 h	Sp + glass
			1228	3 h	Sp + trace Pv + glass
			1227	3 h	Sp + Pv + trace Fo + glass
			1225	18 h	Trace Sp + Pv + Di + glass
57	10	33	1295	3 h	Glass
			1290	3 h	Sp + glass
			1240	2 h	Sp + glass
			1235	2 h	Sp + Pv + glass
			1220	4 h	Sp + Pv + glass
			1215	24 h	Sp + Pv + trace Di + glass
			1200	72 h	Trace Sp + Pv + Di + glass
			1130	7 d	Loose powder (Pv + Di + Mel)

*Assemblage not shown on figure 11.

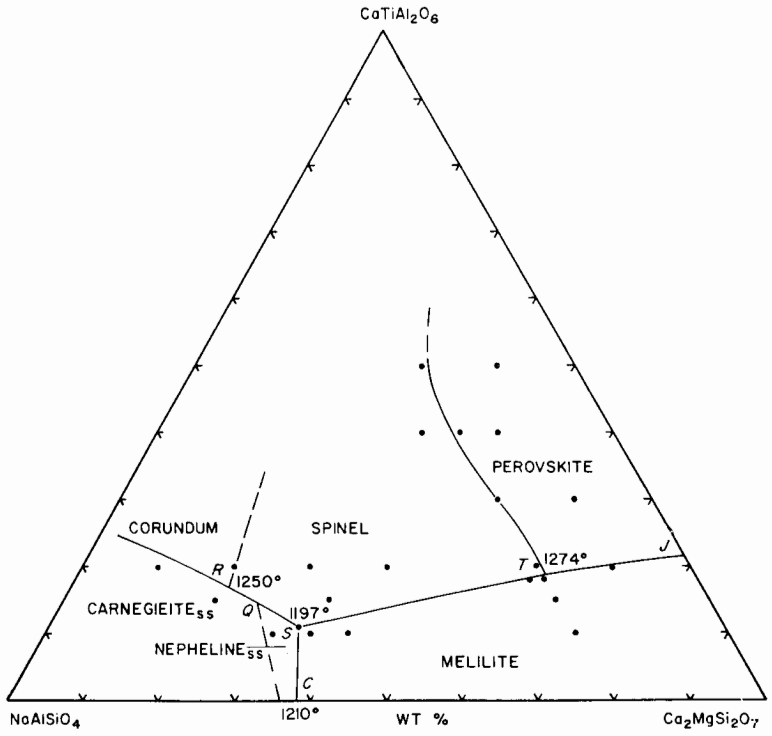

Fig. 5. Liquidus diagram for the join nepheline–akermanite–$CaTiAl_2O_6$.

assemblage is melilite + diopside$_{ss}$ + nepheline$_{ss}$ + liquid. Perovskite and corundum are present in some of the starting mixtures.

On the 10 percent plane (fig. 7) two new four-phase assemblages appear: forsterite + melilite + spinel + liquid at 1175°C (point V) and melilite + spinel + nepheline$_{ss}$ + liquid at 1194°C (point S). Carnegieite$_{ss}$ persists in one of the compositions adjacent to point S ($Di_5Ak_{28}Ne_{57}Tp_{10}$) at temperatures as low as 1180°C. The carnegieite$_{ss}$ is presumably metastable. As Onuma and Yagi (1967) report in the related system akermanite–nepheline, the lower limit of the carnegieite–nepheline inversion temperature occurs at about 1208°C and a composition of $Ne_{80}Ak_{20}$ and is raised in mixtures poorer in $NaAlSiO_4$. Mixtures in the region of point S become a five-phase assemblage with the addition of forsterite to the assemblage nepheline$_{ss}$ + melilite + spinel + liquid. The four-phase assemblage displayed around point V becomes a five-phase assemblage upon the crystallization of nepheline at 1174°C.

Three six-phase assemblages are confirmed in this plane. In the first (1 in fig. 11), perovskite is formed, and spinel is consumed by reaction at about 1160°C. With decreasing temperature the resulting five-

TABLE 4

The join nepheline-akermanite-$CaTiAl_2O_6$

Composition, wt %			Temp, °C	Time	Phases
Ak	Ne	Tp			
70	20	10	1310	3 h	Glass
			1305	18 h	Mel + glass
			1255	18 h	Mel + glass
			1250	18 h	Mel + Pv + glass
			1230	72 h	Mel + Pv + Sp + glass
			1220	72 h	Mel + Pv + Sp + glass
			1210	72 h	Mel + Pv + Sp + Fo + glass
40	50	10	1225	3 h	Glass
			1220	18 h	Mel + glass
			1195	24 h	Mel + glass
			1190	72 h	Mel + Sp + glass
			1185	24 h	Mel + Sp + glass
			1180	24 h	Mel + Sp + Ne + glass
			1175	72 h	Mel + Sp + Ne + glass
			1170	72 h	Mel + Sp + Ne + Fo + glass
35	55	10	1210	3 h	Glass
			1205	18 h	Mel + glass
			1200	3 h	Mel + glass
			1195	24 h	Mel + Ne + trace Sp? + glass
			1175	72 h	Mel + Ne + Sp + glass
			1170	72 h	Mel + Ne + Sp + Fo + glass
30	60	10	1215	3 h	Glass
			1210	3 h	Ne + glass
			1205	72 h	Ne + Sp + glass
			1200	18 h	Ne + Sp + glass
			1195	24 h	Ne + Sp + Mel + glass
33	56	11	1200	3 h	Glass
			1195	18 h	Ne + Sp + Mel + glass
			1175	72 h	Ne + Sp + Mel + Pv? + glass
			1160	96 h	Ne + Mel + Pv + Fo + glass
65	20	15	1295	18 h	Glass
			1290	18 h	Mel + glass
			1285	5 h	Mel + glass
			1280	3 h	Mel + Pv + glass
			1250	18 h	Mel + Pv + glass
			1210	72 h	Mel + Pv + Sp + glass
			1200	18 h	Mel + Pv + Sp + Fo + glass
35	50	15	1225	24 h	Glass
			1220	18 h	Sp + glass
			1200	72 h	Sp + glass
			1195	72 h	Sp + trace Ne + glass
			1190	72 h	Sp + Ne + Mel + Pv + glass
20	65	15	1260	2 h	Glass
			1255	3 h	Trace Cg + glass

TABLE 4 (continued)

Composition, wt %			Temp, °C	Time	Phases
Ak	Ne	Tp			
62	20	18	1290	18 h	Glass
			1285	3 h	Mel + Pv + glass
			1265	72 h	Mel + Pv + glass
			1260	24 h	Mel + Pv + trace Sp + glass
			1190	72 h	Mel + Pv + Sp + glass
			1180	72 h	Mel + Pv + Sp + Fo + glass
60	22	18	1280	3 h	Glass
			1275	3 h	Mel + Pv + glass
			1270	72 h	Mel + Pv + Sp + glass
			1170	96 h	Mel + Pv + Sp + glass
			1160	7 d	Mel + Pv + Sp + Fo + glass
70	10	20	1310	3 h	Glass
			1305	2 h	Mel + Pv + glass
			1280	72 h	Mel + Pv + glass
			1275	15 h	Mel + Pv + Sp + glass
			1205	72 h	Mel + Pv + Sp + glass
			1200	96 h	Mel + Pv + Sp + Fo + glass
60	20	20	1305	2 h	Glass
			1300	18 h	Sp + glass
			1295	2 h	Sp + Pv + glass
			1245	72 h	Sp + Pv + glass
			1240	72 h	Sp + Pv + Mel + glass
			1170	96 h	Sp + Pv + Mel + glass
			1160	7 d	Pv + Mel + Ne + Fo + glass
40	40	20	1275	2 h	Glass
			1270	3 h	Sp + glass
			1245	72 h	Sp + glass
			1240	24 h	Sp + Pv + glass
			1200	18 h	Sp + Pv + glass
			1195	72 h	Sp + Pv + Mel + glass
			1190	72 h	Sp + Pv + Mel + Ne + glass
			1160	96 h	Pv + Mel + Ne + Fo + glass
30	50	20	1280	2 h	Glass
			1275	2 h	Trace Sp + glass
			1235	48 h	Sp + glass
			1230	24 h	Sp + Pv + glass
			1200	18 h	Sp + Pv + glass
			1195	72 h	Sp + Pv + Ne + glass
			1185	72 h	Sp + Pv + Ne + glass
			1180	72 h	Sp + Pv + Ne + Mel + glass
20	60	20	1275	3 h	Glass
			1270	16 h	Cor + Sp + glass
			1240	72 h	Cor + Sp + glass
			1220	48 h	Cor + Sp + Ne + Pv + glass*

TABLE 4 (continued)

Composition, wt %			Temp, °C	Time	Phases
Ak	Ne	Tp			
10	70	20	1320	3 h	Glass
			1315	2 h	Cg + glass
			1270	16 h	Cg + glass
			1265	3 h	Cg + Cor + Pv + glass
			1255	24 h	Cg + Cor? + Sp + Pv + glass*
			1250	24 h	Ne + Cor? + Sp + Pv + glass*
60	10	30	1380	3 h	Glass
			1375	3 h	Pv + glass
			1335	18 h	Pv + glass
			1330	18 h	Pv + Sp + glass
			1220	7 d	Pv + Sp + glass
			1200	96 h	Sp + Pv + Mel + glass
			1160	7 d	Sp + Pv + Mel + Fo + glass
50	20	30	1360	2 h	Glass
			1355	3 h	Sp + Pv + glass
			1250	24 h	Sp + Pv + glass
			1245	72 h	Sp + Pv + Mel + glass
45	15	40	1415	3 h	Glass
			1410	3 h	Pv + glass
			1400	18 h	Pv + glass
			1395	24 h	Pv + trace Sp + glass
40	20	40	1405	2 h	Glass
			1400	3 h	Pv + glass
			1395	24 h	Pv + glass
			1390	18 h	Pv + Sp + glass
			1270	72 h	Pv + Sp + trace Mel + glass
35	25	40	1395	24 h	Glass
			1390	3 h	Sp + glass
			1385	2 h	Sp + Pv + glass
			1265	72 h	Sp + Pv + glass
			1260	72 h	Sp + Pv + Mel + glass
40	10	50	1460	2 h	Trace Pv + glass
			1440	18 h	Pv + glass
			1435	18 h	Pv + trace Sp + glass
			1310	48 h	Pv + Sp + trace Mel + glass
30	20	50	1425	2 h	Glass
			1420	2 h	Sp + glass
			1415	24 h	Sp + glass
			1410	2 h	Sp + Pv + glass
			1305	72 h	Sp + Pv + glass
			1300	72 h	Sp + Pv + Mel + glass

*Assemblage not shown on figure 11.

TABLE 5

The plane diopside-akermanite-nepheline-5 percent $CaTiAl_2O_6$

Composition, wt %			Temp, °C	Time	Phases
Di	Ak	Ne			
20	20	55	1205	2 h	Glass
			1200	2 h	Mel + glass
			1195	2 h	Mel + glass
			1190	2 h	Mel + Ne + glass
			1180	40 h	Mel + Ne + trace Fo + glass
			1150	72 h	Barely fritted cake (Mel + Ne + Di)
35	10	50	1205	15 h	Glass
			1200	2 h	Mel + glass
			1195	2 h	Mel + glass
			1190	72 h	Mel + Fo + glass
			1180	72 h	Mel + Fo + glass
			1175	72 h	Mel + Fo + Ne + glass
			1090	7 d	Fritted cake (Mel + Ne + Di)
			1080	7 d	Loose powder (Mel + Ne + Di)
40	5	50	1190	2 h	Glass
			1185	2 h	Mel + glass
			1180	18 h	Mel + Fo + Ne + glass
45	10	40	1230	2 h	Glass
			1225	2 h	Mel + glass
			1220	15 h	Mel + glass
			1215	18 h	Mel + Fo + glass
			1100	7 d	Fritted cake (Mel + Di + Ne)
			1090	7 d	Loose powder
55	20	20	1290	1-1/2 h	Glass
			1285	1-1/2 h	Mel + glass
			1270	2 h	Mel + glass
			1265	18 h	Mel + Fo + glass
			1190	72 h	Mel + Fo + glass
			1180	40 h	Mel + Fo + Di + glass
			1140	96 h	Mel + Fo + Di + trace Ne + glass
			1135	96 h	Mel + Fo + Di + Ne + glass
			1130	96 h	Mel + Di + Ne + glass
55	10	30	1250	4 h	Glass
			1245	18 h	Fo + glass
			1240	18 h	Fo + Mel + glass
			1150	7 d	Fo + Mel + glass
			1140	96 h	Fo + Mel + Di + glass
			1135	96 h	Mel + Di + glass
			1130	96 h	Mel + Di + Ne + glass
65	20	10	1305	2 h	Glass
			1300	1-1/2 h	Mel + glass
			1285	2 h	Mel + glass
			1280	2 h	Mel + Di + Fo + glass
			1120	120 h	Barely fritted cake
			1110	7 d	Loose powder

TABLE 5 (continued)

Composition, wt %			Temp, °C	Time	Phases
Di	Ak	Ne			
65	5	25	1265	6 h	Glass
			1260	2 h	Fo + glass
			1255	18 h	Fo + glass
			1250	2 h	Fo + Mel + glass
			1150	72 h	Fo + Mel + Di + glass
			1135	96 h	Fo + Mel + Di + Ne + glass
70	15	10	1295	2 h	Glass
			1290	18 h	Mel + Di + glass
			1120	120 h	Fritted cake (Mel + Di + Ne)
			1110	7 d	Loose powder (Mel + Di + Ne)
70	10	15	1280	2 h	Glass
			1275	18 h	Fo + trace Mel + glass
			1260	2 h	Fo + Mel + glass
			1255	4 h	Fo + Mel + Di + glass
			1110	7 d	Barely fritted cake (Mel + Di + Ne)
72	10	13	1290	2 h	Glass
			1285	2 h	Trace Di + glass
			1280	2 h	Di + Fo + Mel + glass

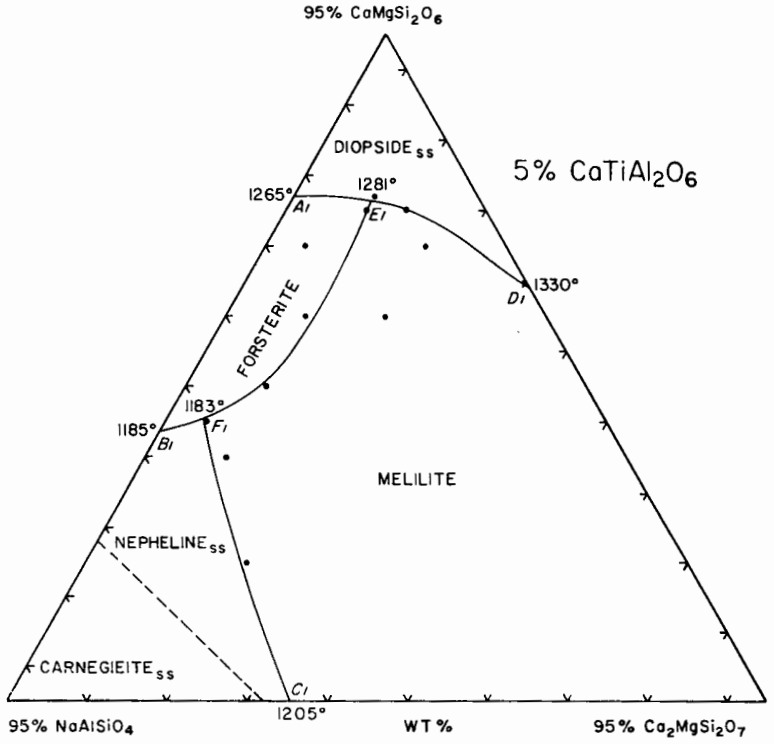

Fig. 6. Liquidus diagram for the plane diopside–akermanite–nepheline–5 percent $CaTiAl_2O_6$.

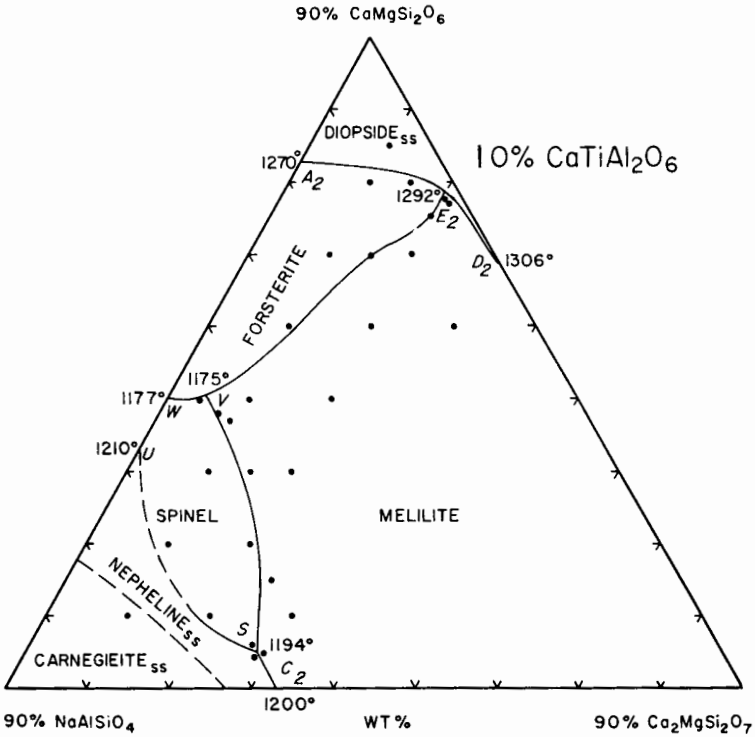

Fig. 7. Liquidus diagram for the plane diopside–akermanite–nepheline–10 percent $CaTiAl_2O_6$.

phase assemblage, fosterite + melilite + nepheline$_{ss}$ + perovskite + liquid, proceeds toward the next reaction (3 in fig. 11), where diopside$_{ss}$ appears and forsterite completely dissolves at approximately 1130°C. The final six-phase assemblage (4 in fig. 11) is indicated by the addition of corundum to the assemblage diopside$_{ss}$ + melilite + nepheline$_{ss}$ + perovskite + liquid at 1100°C. These five crystalline phases constitute a final product in the part of the system under investigation.

Figure 8 shows the plane for 15 percent $CaTiAl_2O_6$. The five-phase and six-phase assemblages present in the 10 percent plane are confirmed in this plane.

Perovskite becomes a primary phase on the 20 percent $CaTiAl_2O_6$ plane (fig. 9). The four-phase assemblage melilite + perovskite + spinel + liquid occurs on the liquidus at T_1. This assemblage is also present in figure 5. The primary field for diopside$_{ss}$ diminishes with increasing $CaTiAl_2O_6$ content and is separated from the melilite field by forsterite in figure 9.

The five-phase assemblage forsterite + melilite + spinel + perovskite + liquid is present in this plane, and with decreasing temperatures it reaches either six-phase assemblages (1) forsterite + melilite + nephe-

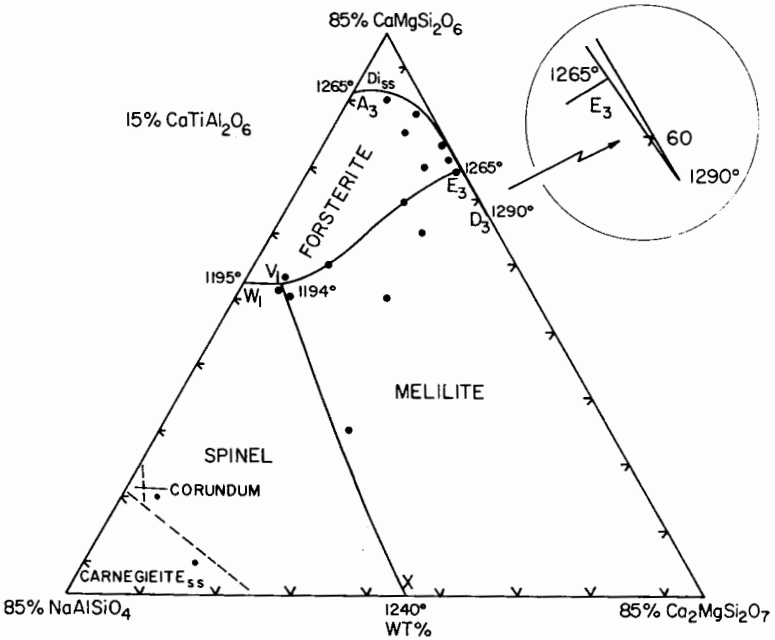

Fig. 8. Liquidus diagram for the plane diopside–akermanite–nepheline–15 percent $CaTiAl_2O_6$.

$line_{ss}$ + spinel + perovskite + liquid or six-phase assemblage (2) forsterite + melilite + spinel + perovskite + $diopside_{ss}$ + liquid (fig. 11). For compositions in the vicinity of points T_1 and V_2 on figure 9 crystallization proceeds to assemblage 2 where spinel is consumed and diopside appears. The resulting assemblage is forsterite + melilite + perovskite + $diopside_{ss}$ + liquid. One composition to the left of this region reaches assemblage (1) where spinel is completely dissolved and $nepheline_{ss}$ begins to crystallize, resulting in the five-phase assemblage forsterite + melilite + perovskite + $nepheline_{ss}$ + liquid. This path was also followed in figure 5.

DIOPSIDE–AKERMANITE–NEPHELINE–$CaTiAl_2O_6$ TETRAHEDRON

The primary phase volumes in the system diopside–akermanite–nepheline–$CaTiAl_2O_6$ are shown in figure 10. The trace of the surface between adjacent primary phase volumes is shown by a solid line. Each line depicts the trace of a surface having two crystalline phases coexisting with liquid—a three phase assemblage. The intersection of three three-phase assemblages results in a four-phase assemblage, having three crystalline phases plus liquid, and these are shown by heavy broken lines. Four four-phase assemblages meeting at a point form a five-phase assemblage.

Two five-phase assemblages are shown in figure 10: V (forsterite + melilite + $nepheline_{ss}$ + spinel + liquid) and Z (forsterite + melilite + perovskite + spinel + liquid). Points V and Z lie on two separate

TABLE 6

The plane diopside-akermanite-nepheline-10 percent $CaTiAl_2O_6$

Composition, wt %			Temp, °C	Time	Phases
Di	Ak	Ne			
5	29	56	1200	1-1/2 h	Trace Mel + glass
			1195	2 h	Mel + glass
			1190	2 h	Mel + Cg + glass
			1185	15 h	Mel + Cg + Sp + glass
			1180	4 h	Mel + Cg + Sp + Ne + glass
			1175	72 h	Mel + Ne + Sp + glass
6	27	57	1200	2 h	Glass
			1195	2 h	Trace Sp + glass
			1190	2 h	Sp + Ne + Mel + glass
10	10	70	1295	1-1/2 h	Glass
			1290	1-1/2 h	Cg + glass
			1225	6 h	Cg + glass
			1220	15 h	Cg + Sp + glass
			1110	7 d	Barely fritted cake
			1100	7 d	Loose powder (Ne + Mel + Pv + Cor)
10	20	60	1235	15 h	Glass
			1230	15 h	Sp + glass
			1225	17 h	Sp + glass
			1220	4 h	Sp + Ne + glass
			1170	72 h	Sp + Ne + glass
			1165	96 h	Sp + Ne + Mel + glass
			1100	7 d	Barely fritted cake
			1090	7 d	Loose powder
10	30	50	1215	2 h	Glass
			1210	1-1/2 h	Mel + glass
			1190	4 h	Mel + glass
			1185	18 h	Mel + Sp + glass
			1180	72 h	Mel + Sp + Ne + glass
			1110	7 d	Barely fritted cake
			1100	7 d	Loose powder
15	25	50	1205	2 h	Glass
			1200	1-1/2 h	Mel + glass
			1195	4 h	Mel + Sp + glass
			1185	18 h	Mel + Sp + glass
			1180	72 h	Mel + Sp + Ne + glass
			1170	96 h	Mel + Sp + Ne + trace Fo + glass
20	10	60	1245	2 h	Glass
			1240	4 h	Trace Sp + glass
			1220	4 h	Sp + glass
			1215	15 h	Sp + Ne + glass
			1175	96 h	Sp + Ne + glass
			1170	96 h	Sp + Ne + Mel + Fo + glass
			1100	7 d	Barely fritted cake (Ne + Mel + Pv + Di)
			1090	7 d	Loose powder
20	20	50	1220	4 h	Glass
			1215	15 h	Sp + glass
			1185	72 h	Sp + glass
			1180	72 h	Sp + Ne + glass

TABLE 6 (continued)

Composition, wt %			Temp, °C	Time	Phases
Di	Ak	Ne			
20	20	50	1175	96 h	Sp + Ne + Mel + glass
			1165	96 h	Sp + Ne + Mel + glass
			1160	96 h	Sp + Ne + Mel + Fo + glass
30	10	50	1200	2 h	Glass
			1195	15 h	Sp + glass
			1185	20 h	Sp + glass
			1180	2 h	Sp + Ne + glass
			1170	72 h	Sp + Ne + glass
			1165	96 h	Sp + Ne + Fo + glass
			1160	48 h	Sp + Ne + Fo + Mel + glass
			1100	7 d	Barely fritted cake
			1090	7 d	Loose powder
30	15	45	1205	15 h	Glass
			1200	15 h	Mel + glass
			1180	1-1/2 h	Mel + glass
			1175	72 h	Mel + Sp + glass
			1170	2 h	Mel + Sp + Fo + glass
30	20	40	1220	15 h	Glass
			1215	4 h	Mel + glass
			1190	4 h	Mel + glass
			1185	72 h	Mel + Fo + glass
			1180	72 h	Mel + Fo + glass
			1175	72 h	Mel + Fo + Sp + glass
			1165	96 h	Mel + Fo + Sp + glass
			1160	96 h	Mel + Fo + Ne + glass
37	9	44	1200	1-1/2 h	Glass
			1195	15 h	Trace Mel + glass
			1180	4 h	Mel + glass
			1175	2 h	Mel + Fo + glass
			1170	72 h	Mel + Fo + Sp + glass
38	7	45	1190	3 h	Glass
			1185	2 h	Mel + Sp + glass
			1180	2 h	Mel + Sp + glass
			1175	2 h	Mel + Sp + Fo + glass
			1170	96 h	Mel + Sp + Fo + Ne + glass
			1165	96 h	Mel + Sp + Fo + Ne + glass
			1160	96 h	Mel + Fo + Ne + Pv + glass
40	4	46	1180	2 h	Trace Sp + glass
			1175	4 h	Sp + Mel + trace Fo + trace Ne + glass
			1170	15 h	Sp + Mel + Fo + Ne + glass
			1165	96 h	Sp + Mel + Fo + Ne + glass
			1160	96 h	Mel + Fo + Ne + Pv + glass
40	10	40	1200	2 h	Glass
			1195	15 h	Mel + Fo + glass
			1165	96 h	Mel + Fo + glass
			1160	48 h	Mel + Fo + Ne + glass
			1100	7 d	Barely fritted cake (Mel + Ne + Di + Pv)
			1090	7 d	Loose powder (Di + Mel + Ne + Pv + Cor?)

TABLE 6 (continued)

Composition, wt %			Temp, °C	Time	Phases
Di	Ak	Ne			
40	20	30	1245	18 h	Glass
			1240	2 h	Mel + glass
			1225	18 h	Mel + glass
			1220	18 h	Mel + Fo + glass
42	8	40	1205	1-1/2 h	Glass
			1200	2 h	Mel + glass
			1195	18 h	Mel + glass
			1190	2 h	Mel + Fo + glass
			1165	96 h	Mel + Fo + glass
			1160	96 h	Mel + Fo + Ne + Pv + glass
			1130	96 h	Mel + Ne + Pv + Di + glass
50	10	30	1235	2 h	Glass
			1230	2 h	Trace Fo + glass
			1225	18 h	Fo + glass
			1220	18 h	Fo + Mel + glass
			1170	48 h	Fo + Mel + glass
			1160	72 h	Fo + Mel + Di + glass
			1140	96 h	Trace Fo + Mel + Di + trace Pv + glass
			1130	96 h	Mel + Di + Pv + glass
50	20	20	1265	18 h	Glass
			1260	2 h	Mel + glass
			1255	2 h	Mel + glass
			1250	2 h	Mel + trace Fo + glass
			1185	20 h	Mel + Fo + glass
			1180	72 h	Mel + Fo + Di + glass
			1170	72 h	Mel + trace Fo + Di + glass
			1150	96 h	Mel + Di + glass
			1140	96 h	Mel + Di + Pv + glass
50	30	10	1310	2 h	Glass
			1305	2 h	Mel + glass
			1285	2 h	Mel + glass
			1280	2 h	Mel + trace Fo + glass
			1240	72 h	Mel + Fo + glass
			1235	72 h	Mel + Fo + Di + glass
			1170	72 h	Mel + Di + Pv + glass
			1100	7 d	Barely fritted cake
			1090	7 d	Loose powder
60	10	20	1260	18 h	Glass
			1255	18 h	Fo + glass
			1250	2 h	Fo + glass
			1245	18 h	Fo + trace Mel + glass
			1200	15 h	Fo + Mel + glass
			1195	18 h	Fo + Mel + Di + glass
			1170	72 h	Mel + Di + glass
			1090	7 d	Barely fritted cake (Mel + Di + Ne + Pv)
60	15	15	1270	1-1/2 h	Glass
			1265	1-1/2 h	Mel + trace Fo + glass
			1110	9 d	Barely fritted cake
			1100	7 d	Loose powder

TABLE 6 (continued)

Composition, wt %			Temp, °C	Time	Phases
Di	Ak	Ne			
60	20	10	1290	18 h	Glass
			1285	2 h	Mel + glass
			1280	2 h	Mel + glass
			1275	2 h	Mel + Fo + glass
			1260	18 h	Mel + Fo + glass
			1255	18 h	Mel + Fo + trace Di + glass
			1170	72 h	Mel + Di + glass
			1110	7 d	Barely fritted cake
			1100	7 d	Loose powder
65	20	5	1300	4 h	Glass
			1295	4 h	Mel + Fo + glass
			1280	2 h	Mel + Fo + glass
			1275	4 h	Mel + Fo + Di + glass
67	21	2	1315	1-1/2 h	Glass
			1310	15 h	Trace Mel + glass
			1305	1-1/2 h	Mel + glass
			1300	3 h	Mel + Fo + trace Di + glass
			1230	96 h	Mel + trace Fo + Di + glass
			1225	96 h	Mel + Di + Pv + glass
68	20	2	1315	2 h	Glass
			1310	2 h	Mel + glass
			1305	1-1/2 h	Mel + Fo + glass
			1295	3 h	Mel + Fo + glass
			1290	15 h	Mel + Fo + Di + glass
			1230	96 h	Mel + trace Fo + Di + glass
			1200	96 h	Loose powder (Mel + Di + Ne + Pv?)
70	10	10	1290	18 h	Glass
			1285	2 h	Trace Fo + glass
			1265	18 h	Fo + glass
			1260	18 h	Fo + Di + glass
			1255	18 h	Fo + Di + Mel + glass
			1100	7 d	Barely fritted cake (Di + Mel + Pv + Ne)
			1090	7 d	Loose powder (Di + Mel + Pv + Ne)
75	10	5	1315	1-1/2 h	Trace Di + glass
			1290	3 h	Di + glass
			1285	18 h	Di + Fo + trace Mel + glass
			1230	96 h	Di + trace Fo + Mel + glass
			1225	96 h	Di + Mel + glass
			1110	7 d	Fritted cake
			1100	7 d	Loose powder
70	15	5	1300	2 h	Glass
			1295	4 h	Fo + glass
			1290	15 h	Fo + trace Di + glass
			1285	3 h	Fo + Di + Mel + glass

*Metastable (?); Ne should be the stable form (see Onuma and Yagi, 1967).

TABLE 7

The plane diopside-akermanite-nepheline-15 percent $CaTiAl_2O_6$

Composition, wt %			Temp, °C	Time	Phases
Di	Ak	Ne			
5	15	65	1290	2 h	Glass
			1280	2 h	Cg + glass
			1270	2 h	Cg + glass
			1260	2 h	Cg + Sp + glass
			1250	2 h	Cg + Sp + trace Cor + glass
			1230	2 h	Cg + Sp + Cor + glass
15	5	65	1300	2 h	Glass
			1290	2 h	Sp + glass
			1280	2 h	Sp + glass
			1270	2 h	Sp + Cg + glass
			1260	2 h	Sp + Cg + glass
			1250	2 h	Sp + Cg + Ne + Cor + glass
25	25	35	1230	18 h	Glass
			1225	2 h	Mel + glass
			1220	2 h	Mel + Sp + glass
			1200	96 h	Mel + Sp + glass
			1190	96 h	Mel + Sp + Pv + glass
45	7	33	1200	1-1/2 h	Glass
			1195	2 h	Mel + trace Sp + glass
			1190	15 h	Mel + Sp + Fo + glass
			1180	1-1/2 h	Mel + Sp + Fo + glass
			1175	4 h	Mel + Sp + Fo + Pv + glass
			1160	72 h	Mel + Sp + Fo + Pv + glass
			1155	96 h	Mel + Fo + Pv + Ne + glass
45	20	20	1255	3 h	Glass
			1250	2 h	Mel + glass
			1230	18 h	Mel + glass
			1225	4 h	Mel + Fo + glass
			1215	2-1/2 h	Mel + Fo + glass
			1210	18 h	Mel + Fo + Pv + glass
46	5	34	1205	2 h	Glass
			1200	2 h	Sp + glass
			1195	15 h	Sp + trace Fo + glass
			1190	1-1/2 h	Sp + Fo + Mel + glass
			1175	4 h	Sp + Fo + Mel + glass
			1170	18 h	Sp + Fo + Mel + Pv + glass
			1155	96 h	Fo + Mel + Pv + Ne + glass
48	5	32	1205	4 h	Glass
			1200	2 h	Fo + glass
			1195	15 h	Fo + Mel + trace Sp + glass
			1160	72 h	Fo + Mel + Sp + Pv + glass
			1155	96 h	Fo + Mel + Pv + Ne + glass
50	10	25	1225	18 h	Glass
			1220	2 h	Mel + Fo + glass
			1190	72 h	Mel + Fo + glass
			1180	72 h	Mel + Fo + Sp + glass
55	20	10	1290	1-1/2 h	Glass
			1285	1-1/2 h	Mel + glass
			1275	18 h	Mel + glass
			1270	2 h	Mel + Fo + glass
			1220	24 h	Mel + Fo + glass
			1215	72 h	Mel + Fo + trace Di + glass
			1160	72 h	Mel + trace Fo + Di + glass
			1110	9 d	Fritted cake
			1100	7 d	Loose powder

TABLE 7 (continued)

Composition, wt %			Temp, °C	Time	Phases
Di	Ak	Ne			
60	15	10	1265	2 h	Glass
			1260	15 h	Fo + Mel + glass
			1220	48 h	Fo + Mel + glass
			1215	72 h	Fo + Mel + Di + glass
			1160	72 h	Trace Fo + Mel + Di + glass
64	20	1	1295	1-1/2 h	Glass
			1290	1-1/2 h	Mel + Fo + glass
			1270	2 h	Mel + Fo + glass
			1265	2 h	Mel + Fo + trace Di + glass
			1240	4 h	Mel + trace Fo + Di + glass
			1230	48 h	Mel + Di + Pv + glass
65	15	5	1285	1 h	Glass
			1280	2 h	Fo + Mel + glass
			1265	20 h	Fo + Mel + glass
			1260	4 h	Fo + Mel + Di + glass
			1190	72 h	Mel + Di + trace Pv + glass
66	18	1	1295	1-1/2 h	Glass
			1290	1-1/2 h	Fo + glass
			1285	2 h	Fo + Mel + glass
			1275	15 h	Fo + Mel + glass
			1270	15 h	Fo + Mel + Di + glass
			1230	48 h	Mel + Di + Pv + glass
68	16	1	1300	1 h	Glass
			1295	1 h	Fo + glass
			1280	2 h	Fo + glass
			1275	2 h	Fo + Mel + glass
			1270	15 h	Fo + Mel + Di + glass
			1230	48 h	Trace Fo + Mel + Di + Pv + glass
70	10	5	1290	1-1/2 h	Glass
			1285	1-1/2 h	Fo + glass
			1270	2 h	Fo + glass
			1265	18 h	Fo + Mel + glass
			1260	18 h	Fo + Mel + glass
			1255	3 h	Fo + Mel + Di + glass
			1200	72 h	Trace Fo + Mel + Di + glass
			1190	72 h	Mel + Di + Pv + glass
			1130	7 d	Fritted cake (Mel + Di + Pv)
			1120	7 d	Loose powder
73	10	2	1300	1 h	Glass
			1295	1 h	Fo + glass
			1280	1 h	Fo + glass
			1275	2 h	Fo + Di + glass
			1270	2 h	Fo + Di + glass
			1265	3 h	Fo + Di + Mel + glass
			1130	7 d	Fritted cake (Mel + Di + Pv)
			1120	7 d	Loose powder
75	5	15	1295	1 h	Glass
			1290	1-1/2 h	Fo + glass
			1265	18 h	Fo + glass
			1260	18 h	Fo + Di + glass
			1255	3 h	Fo + Di + Mel + glass
			1190	72 h	Trace Fo + Di + Mel + Pv + glass
			1130	7 d	Fritted cake (Mel + Di + Pv + Ne)
			1120	7 d	Loose powder

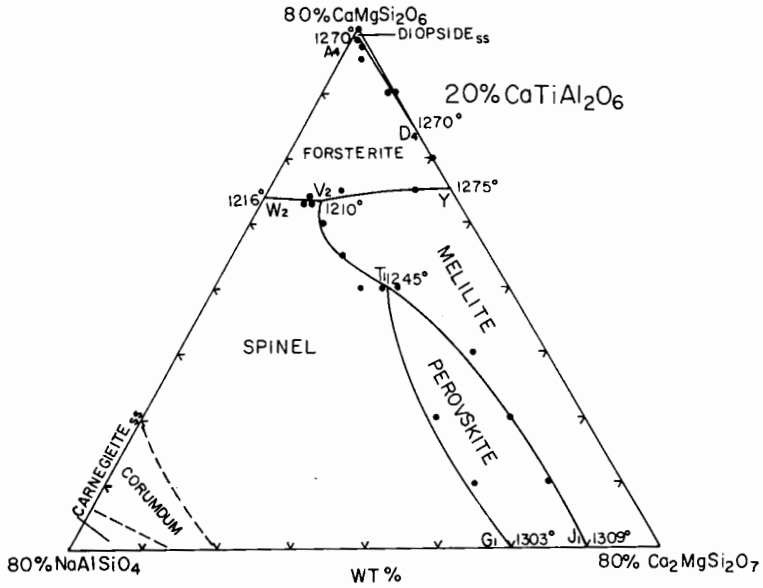

Fig. 9. Liquidus diagram for the plane diopside–akermanite–nepheline–20 percent $CaTiAl_2O_6$.

lines, showing five-phase assemblages that meet together with three other similar lines. Thus V and Z of figure 10 may behave like piercing points for the five component system. Six additional five-phase assemblages (table 9) have been confirmed in the main part of the system, but they are not shown on figure 10 as they may lie outside the tetrahedron.

COURSES OF CRYSTALLIZATION

As the number of the component oxides of the system under investigation is six (Na_2O–CaO–MgO–Al_2O_3–TiO_2–SiO_2), the system may actually be a six-component system. However, the number of crystalline phases, most of which are solid solutions, never exceed five in any assemblage, and their melting interval is small, and consequently the system behaves like a five-component system for which a flow sheet has been constructed (fig. 11). The lines, showing five-phase assemblages, are actually divariant phase assemblages, and the points 1, 2, 3, and 4 are not points with definite temperatures, but sections of lines with temperature ranges representing univariant or six-phase assemblages in a six-component system. Of these 1, 2, and 3 show reaction relations, and 4 shows a eutectic relation.

Six-phase assemblage (1).—All five of the five-phase assemblages which evolve from (1) were observed experimentally. They are forsterite + melilite + nepheline_{ss} + spinel + liquid, melilite + nepheline_{ss} + spinel + perovskite + liquid, forsterite + melilite + spinel + perovskite + liquid, forsterite + melilite + nepheline_{ss} + perovskite + liquid, and forsterite + nepheline_{ss} + spinel + perovskite + liquid.

TABLE 8

The plane diopside-akermanite-nepheline-20 percent $CaTiAl_2O_6$

Composition, wt %			Temp, °C	Time	Phases
Di	Ak	Ne			
10	50	20	1305	20 h	Glass
			1300	18 h	Pv + glass
			1290	2 h	Pv + Sp + Mel + glass
20	40	20	1275	72 h	Glass
			1270	72 h	Pv + glass
			1265	48 h	Pv + Sp + Mel + glass
			1205	40 h	Pv + Sp + Mel + glass
			1200	76 h	Pv + Sp + Mel + trace Fo + glass
			1130	7 d	Fritted cake (Pv + Mel + Di + Ne)
			1120	7 d	Loose powder
20	50	10	1310	2 h	Glass
			1305	20 h	Mel + Pv + glass
			1265	48 h	Mel + Pv + trace Sp + glass
			1245	72 h	Mel + Pv + Sp + glass
			1240	48 h	Mel + Pv + Sp + Fo + glass
			1130	7 d	Fritted cake (Mel + Pv + Di + Ne)
			1120	7 d	Loose powder
30	40	10	1295	2 h	Glass
			1290	18 h	Mel + glass
			1285	17 h	Mel + glass
			1280	20 h	Mel + Pv + glass
			1260	24 h	Mel + Pv + glass
			1255	48 h	Mel + Pv + Sp + glass
			1245	48 h	Mel + Pv + Sp + glass
			1240	48 h	Mel + Pv + Sp + Fo + glass
			1160	7 d	Mel + Pv + Di + glass
			1130	7 d	Fritted cake (Mel + Pv + Di + Ne)
			1120	7 d	Loose powder
10	10	60	1300	2 h	Glass
			1290	4 h	Sp + glass
			1260	4 h	Sp + trace Pv + glass
			1250	4 h	Sp + Pv + trace Cg + glass
40	10	30	1275	2 h	Glass
			1270	18 h	Trace Sp + glass
			1225	48 h	Sp + glass
			1220	96 h	Sp + Pv + glass
			1190	96 h	Sp + Pv + glass
			1185	7 d	Sp + Pv + Mel + glass
			1180	7 d	Sp + Pv + Mel + glass
			1175	7 d	Sp + Pv + Mel + Fo + glass
			1165	7 d	Sp + Pv + Mel + Fo + glass
			1160	7 d	Pv + Mel + Fo + Ne + glass
			1120	7 d	Barely fritted cake
			1110	7 d	Loose powder
40	23	17	1255	24 h	Glass
			1250	24 h	Trace Sp + glass
			1245	24 h	Sp + Mel + Pv + glass
			1230	48 h	Sp + Mel + Pv + glass
			1220	5 d	Sp + Mel + Pv + Fo + glass
			1160	7 d	Mel + Pv + Fo + Di + glass

TABLE 8 (continued)

Composition, wt %			Temp, °C	Time	Phases
Di	Ak	Ne			
40	20	20	1265	2 h	Glass
			1260	72 h	Sp + glass
			1235	72 h	Sp + glass
			1230	72 h	Sp + Pv + glass
			1215	72 h	Sp + Pv + glass
			1210	72 h	Sp + Pv + Mel + Fo + glass
			1170	7 d	Sp + Pv + Mel + Fo + glass
			1165	7 d	Trace Sp + Pv + Mel + Fo + Di + glass
			1160	7 d	Pv + Mel + Fo + Di + glass
			1130	7 d	Fritted cake (Pv + Mel + Di + Ne)
			1120	7 d	Loose powder
40	25	15	1260	2 h	Glass
			1255	2 h	Mel + glass
			1250	16 h	Mel + glass
			1245	20 h	Mel + Pv + glass
			1240	18 h	Mel + Pv + Sp + glass
			1230	16 h	Mel + Pv + Sp + glass
			1225	72 h	Mel + Pv + Sp + Fo + glass
			1185	7 d	Mel + Pv + Sp + Fo + glass
			1180	7 d	Mel + Pv + Fo + Di + glass
			1170	7 d	Mel + Pv + Fo + Di + glass
			1165	7 d	Mel + Pv + Di + glass
45	15	20	1235	24 h	Glass
			1230	24 h	Sp + Mel + glass
			1225	24 h	Sp + Mel + Pv + glass
			1220	24 h	Sp + Mel + Pv + Fo + glass
			1160	96 h	Mel + Pv + Di + glass
50	10	20	1260	2 h	Glass
			1255	2 h	Mel + glass
			1225	48 h	Mel + glass
			1220	2 h	Mel + Pv + Fo + glass
			1200	96 h	Mel + Pv + Fo + glass
			1195	96 h	Mel + Pv + Fo + Sp + glass
			1190	96 h	Mel + Pv + Fo + Di + glass
			1165	7 d	Mel + Pv + trace Fo + Di + glass
53	6	21	1260	18 h	Glass
			1255	4 h	Trace Sp + glass
			1250	18 h	Sp + Mel + Fo + glass
			1210	48 h	Sp + Mel + Fo + glass
			1200	20 h	Sp + Mel + Fo + Pv + glass
52	5	23	1250	4 h	Trace Sp + glass
			1230	18 h	Sp + glass
			1225	24 h	Sp + Fo + glass
			1210	24 h	Sp + Fo + trace Mel + glass
			1205	48 h	Sp + Fo + Mel + glass
			1200	48 h	Sp + Fo + Pv + Mel + glass
			1190	72 h	Sp + Fo + Pv + Mel + glass
			1180	72 h	Sp + Fo + Pv + Mel + Di + glass
			1175	7 d	Trace Sp + Fo + Pv + Mel + Di + glass
			1170	72 h	Fo + Pv + Mel + Di + glass
			1160	72 h	Pv + Mel + Di + glass

TABLE 8 (continued)

Composition, wt %			Temp, °C	Time	Phases
Di	Ak	Ne			
54	6	20	1225	2 h	Glass
			1220	2 h	Fo + glass
			1210	18 h	Fo + glass
			1205	96 h	Fo + Sp + Mel + glass
			1200	72 h	Fo + Sp + Mel + glass
			1195	96 h	Fo + Sp + Mel + Pv + glass
			1180	72 h	Fo + Sp + Mel + Pv + glass
			1175	7 d	Fo + Mel + Pv + Di + glass
			1170	72 h	Fo + Mel + Pv + Di + glass
			1160	72 h	Mel + Pv + Di + glass
55	10	15	1245	2 h	Glass
			1240	3 h	Trace Fo + glass
			1235	16 h	Fo + glass
			1230	2 h	Fo + Mel + glass
			1215	72 h	Fo + Mel + glass
			1210	72 h	Fo + Mel + Pv + glass
			1190	72 h	Fo + Mel + Pv + glass
			1185	7 d	Fo + Mel + Pv + Di + glass
			1170	72 h	Trace Fo + Mel + Pv + Di + glass
55	20	5	1275	2 h	Glass
			1270	2 h	Mel + Fo + glass
			1230	24 h	Mel + Fo + glass
			1225	18 h	Mel + Fo + Pv + glass
			1220	24 h	Mel + Fo + Pv + Di + glass
			1205	96 h	Mel + Fo + Pv + Di + glass
			1200	72 h	Mel + Pv + Di + glass
70	9	1	1295	2 h	Glass
			1290	2 h	Fo + glass
			1255	72 h	Fo + glass
			1250	2 h	Fo + Di + glass
			1230	72 h	Fo + Di + Mel + glass
			1225	72 h	Di + Mel + Pv + glass
75	3	2	1295	2 h	Glass
			1290	18 h	Trace Fo + glass
			1260	2 h	Fo + glass
			1255	2 h	Fo + Di + glass
			1225	72 h	Fo + Di + glass
			1220	96 h	Di + Pv + glass
			1205	72 h	Di + Pv + trace Mel + glass
77	2	1	1300	2 h	Glass
			1295	2 h	Trace Fo + glass
			1265	2 h	Fo + glass
			1260	2 h	Fo + Di + glass
78	1	1	1305	2 h	Glass
			1300	2 h	Fo + glass
			1265	6 h	Fo + glass
			1260	16 h	Fo + Di + glass

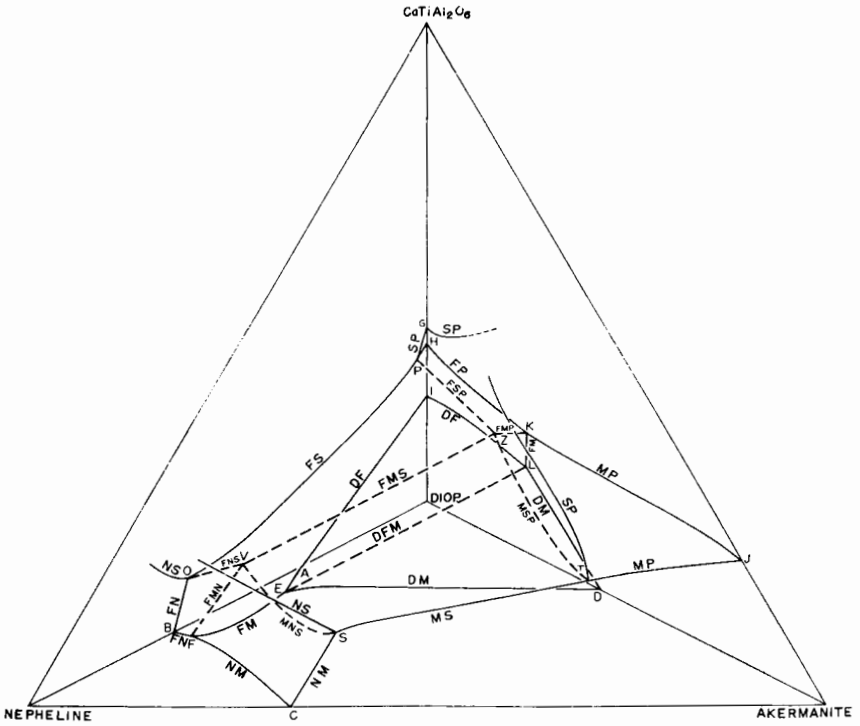

Fig. 10. Tetrahedron representing liquidus phase volumes in the system diopside–akermanite–nepheline–$CaTiAl_2O_6$. Relations are explained in the text. D = diopside, F = forsterite, M = melilite, N = nepheline, P = perovskite, S = spinel.

At (1) spinel disappears as the result of its reaction with liquid. This reaction is demonstrated in three of the four possible assemblages. Crystallization of forsterite, melilite, $nepheline_{ss}$, and spinel from liquid with falling temperature reaches (1), and spinel begins to react with simultaneous crystallization of perovskite. A second five-phase assemblage passes through Z at 1215°C with crystallization of forsterite, melilite, spinel, and perovskite, and also reaches (1). In this assemblage spinel disappears, and $nepheline_{ss}$ begins to crystallize. A third five-phase assemblage (spinel + melilite + $nepheline_{ss}$ + perovskite + liquid) reaches (1) with concomitant crystallization of forsterite and disappearance of spinel. A fourth assemblage (forsterite + $nepheline_{ss}$ + spinel + perovskite + liquid) should also meet at (1), but crystallization beyond the five-phase assemblage was not confirmed in the present investigation.

These five-phase assemblages meet at (1) at a temperature of 1165°C to 1155°C and yield a new five-phase assemblage, forsterite, melilite, $nepheline_{ss}$, and perovskite which crystallizes with falling temperature toward (3).

Six-phase assemblage (2).—This reaction, marked by the disappearance of spinel and formation of $diopside_{ss}$ has considerable temperature

TABLE 9

Five-phase and six-phase assemblages in the system diopside-akermanite-nepheline-$CaTiAl_2O_6$*

Five-phase assemblages	Six-phase assemblages
Mel + Ne + Sp + Pv + liquid	Fo + Mel + Ne + Sp + Pv + liquid
Fo + Ne + Sp + Pv + liquid	
Fo + Mel + Ne + Sp + liquid	Fo + Mel + Sp + Pv + Di + liquid
Fo + Mel + Sp + Pv + liquid	Di + Fo + Mel + Ne + Pv + liquid
Fo + Mel + Ne + Pv + liquid	
Di + Fo + Mel + Pv + liquid	Di + Mel + Ne + Pv + Cor + liquid
Di + Fo + Mel + Ne + liquid	
Di + Mel + Ne + Pv + liquid	

*Only assemblages used to construct figure 11 are listed.

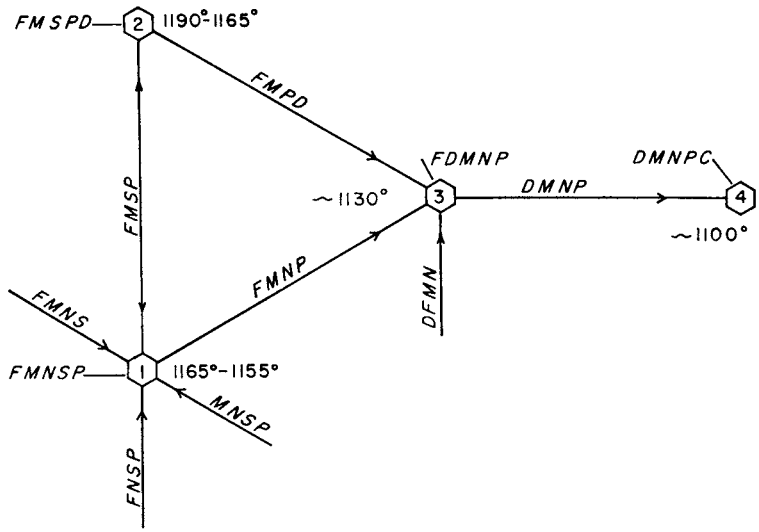

Fig. 11. Mutual relations of five-phase and six-phase assemblages in the system diopside–akermanite–nepheline–$CaTiAl_2O_6$. Full explanation in the text. Abbreviations: C = corundum; the remainder are the same as in figure 10. Liquid not shown.

range (1190°C-1165°C). Two five-phase assemblages which meet at (2) as shown in figure 11 were found. The assemblage forsterite + spinel + melilite + perovskite + liquid occurs between (1) and (2). With falling temperature this assemblage proceeds either to (1) or (2). Beyond point (2) the assemblage forsterite + melilite + perovskite + $diopside_{ss}$ + liquid crystallizes toward reaction point (3).

Six-phase assemblage (3).—The third reaction, marked by the disappearance of forsterite, is reached at about 1130°C. Four of the five five-phase assemblages which meet at (3) were confirmed (fig. 11).

The assemblage forsterite + melilite + $nepheline_{ss}$ + perovskite + liquid occurs between (1) and (3), and between (2) and (3) is the

assemblage forsterite + melilite + perovskite + diopside$_{ss}$ + liquid. With falling temperature these assemblages reach the third reaction. After forsterite is completely consumed, crystallization of diopside$_{ss}$ + melilite + nepheline$_{ss}$ + perovskite proceeds with decreasing temperature toward (3).

In addition to these, one other five-phase assemblage, diopside$_{ss}$ + forsterite + melilite + nepheline$_{ss}$ + liquid, was observed. This assemblage is generated from the basal join diopside–akermanite–nepheline and has petrological significance as will be stated later.

Six-phase assemblage (4).—From the phase assemblages of the starting materials and the beginning of melting data, this is assumed to be one of the main goals of crystallization in the system diopside–akermanite–nepheline–$CaTiAl_2O_6$. The five-phase assemblage diopside$_{ss}$ + melilite + nepheline$_{ss}$ + perovskite + liquid generated from (3) may be joined by corundum. The liquid is consumed at about 1100°C, the lowest temperature at which liquid is observed in this system.

CRYSTALLINE PHASES

All the crystalline phases obtained in the present system with the possible exception of perovskite, spinel, and corundum are solid solutions of variable composition.

Perovskite, spinel, and corundum.—These three phases are regarded as having definite, or essentially definite compositions, as their X-ray diffraction reflections are constant in all of the compositions studied. Perovskite occurs mainly in minute octahedral or irregular crystals, slightly brownish in color. It is easily identified by its extremely high refractive index. Spinel forms small octahedral crystals and is easily distinguished from corundum by its isotropic nature and octahedral form. Corundum occurs mainly as minute irregular crystals, but it shows a hexagonal cross section near the liquidus.

Nepheline$_{ss}$ and carnegieite$_{ss}$.—Nepheline$_{ss}$ occurs in hexagonal plates or stout prismatic forms and has somewhat higher refractive indices than pure nepheline. Carnegieite$_{ss}$ shows typical fish egg form, commonly exhibiting the characteristic polysynthetic twinning. A slight shift is observed in the powder X-ray diffraction patterns of both nepheline$_{ss}$ and carnegieite$_{ss}$, as compared with those of pure crystals. The nepheline–carnegieite inversion takes place over a rather wide range of temperatures as shown elsewhere (Onuma and Yagi, 1967). Thus nepheline and carnegieite are not pure compounds but solid solutions of undermined composition. Metastable persistence of carnegieite$_{ss}$ to temperatures as low as 1180°C is suggested for at least one composition (see table 6). This temperature is considerably lower than the minimum inversion temperature of 1208°C found by Onuma and Yagi (1967) in the analogous system akermanite–nepheline.

Melilite.—Melilite mainly has a tetragonal habit, but it also forms small granular, rounded crystals. The birefringence varies from low to

nearly isotropic, indicating that the melilite is not pure akermanite but a solid solution of variable composition. Soda-melilite molecule, $NaCaAlSi_2O_7$, and gehlenite molecule, $CaAl_2SiO_7$, are both probably incorporated in the melilite as discussed previously by Onuma and Yagi (1967). The titanium content in natural melilites is generally very low and never exceeds 0.7 wt percent TiO_2 even in those from TiO_2-rich nephelinites or related rocks (Deer, Howie, Zussman, 1962). Therefore synthetic melilite in this system is presumably very low in Ti, though the exact composition remains unknown.

Forsterite.—Forsterite usually occurs in colorless rounded forms, showing high retardation. Near its liquidus temperatures, however, forsterite forms faceted stout prismatic crystals. The refractive indices of the forsterite obtained from some mixtures are $\alpha = 1.636$ and $\gamma = 1.673$, which is nearly pure forsterite in composition. A small amount of the monticellite molecule ($CaMgSiO_4$) may be present in solid solution although its presence is not established.

Diopside.—Diopside$_{ss}$ forms stout prismatic crystals rarely twinned on (100) near the liquidus, but forms rounded grains when coexisting with melilite, perovskite, and nepheline$_{ss}$ at lower temperatures. The diopside$_{ss}$ is always colorless and shows oblique extinction. Its optical properties and unit-cell dimensions for the join diopside–$CaTiAl_2O_6$ have been determined by Yagi and Onuma (1967) and Onuma, Hijikata, and Yagi (1968). When diopside$_{ss}$ coexists with other phases in the subsolidus region in the system diopside–akermanite–nepheline–$CaTiAl_2O_6$, its refractive indices are $\alpha = 1.680$ and $\gamma = 1.715$, indicating the diopside$_{ss}$ has almost the maximum content of $CaTiAl_2O_6$ molecule in solid solution. The diopside$_{ss}$ in this system incorporates up to 4 wt percent TiO_2 before perovskite appears. This diopside$_{ss}$ is colorless in spite of the comparatively high titanium content and contrasts with the commonly pleochroic natural titanaugites. The pleochroism thus cannot be ascribed to Ti^{4+}; instead it may be caused by the presence of Ti^{3+} (Smith and Cohen, 1963), Fe^{2+}, Fe^{3+}, or some combination of these ions.

PETROLOGICAL IMPLICATIONS

Titanaugites and Related Pyroxenes

Of the various silicates crystallizing in the present system, diopside$_{ss}$ is the only silicate that contains an appreciable amount of titanium, whereas forsterite, melilite, nepheline$_{ss}$, and carnegieite$_{ss}$ have little or none. Perovskite is the only titanium-bearing oxide present. This partition of titanium is in agreement with the observations on undersaturated, alkali basaltic rocks formed at high temperatures, in which iron-titanium oxides have not yet crystallized out or are present in small amounts.

Recently Aoki (1967) classified the alkali basalt magmas on the basis of the mafic mineral assemblage and order of crystallization into a higher-temperature type in which titanaugite is associated with titano-

magnetite and a lower-temperature type in which titanaugite, kaersutite, and titanbiotite are associated with titanomagnetite. The role of titanium in the first type can be explained by the phase equilibria relations in the present system in so far as it is concerned with the early stage prior to the separation of titanomagnetite. The behavior of titanium in the second type is beyond the scope of the present investigation because of the importance of hydrous silicates and role of water in the partitioning of titanium.

Figure 2 indicates that the diopside$_{ss}$ separating from the liquid as primary phases in the investigated system show gradual enrichment in TiO_2 with crystallization. This compositional variation is similar to that occuring in titanaugites or titan-bearing pyroxenes crystallizing in the early stages from feldspar-bearing alkali basaltic rocks as shown by the following examples. Lack of detailed studies of natural materials precludes comparison with the pyroxenes from nephelinites or melilite nephelinites. In Morotu alkalic rocks, the evolution of pyroxenes is from diopsidic augite poor in TiO_2, through titanaugite with 2.7 to 2.9 percent TiO_2, to aegirine with 0.6 percent TiO_2 (Yagi, 1953). A similar trend is also found in Iki alkalic rocks (Aoki, 1959, 1964), Atumi dolerite (Kushiro, 1964), and Takakusayama alkalic rocks (Tiba, 1966). In the Hocheifel alkali basaltic rocks, the titanium content of pyroxenes increase with advancing crystallization (Huckenholz, 1965a, b, and 1966).

Verhoogen (1962) has indicated that high oxygen partial pressure favors the concentration of titanium in silicates.[1] Yagi (1966) has suggested that on the basis of stability relations of acmite pyroxenes, oxygen partial pressure increases with fractionation in many basaltic magmas. However, titanium does not always enter silicates preferentially in the later stages when P_{O_2} becomes high.

Thus the increase of titanium in natural pyroxenes in the early stage is substantiated by the equilibria relations in the join diopside–$CaTiAl_2O_6$ (fig. 2). In the middle or later stage when the titanium is also distributed in other silicate and oxide phases, the relations are too complicated to be estimated from the simplified system.

Evolution of Alkali Basaltic Magmas

Schairer and Yoder (1964) studied the quaternary system nepheline–forsterite–silica–larnite and found that in the undersaturated part the parental liquid may be represented either by olivine nephelinite or olivine melilitite. These liquids fractionate toward olivine melilite nephelinite, melilite nephelinite, and wollastonite melilite nephelinite. Titanium was not included in this simplified basalt system. In the present system perovskite crystallizes instead of wollastonite, thus representing natural rocks more closely.

A number of naturally occurring mafic alkalic rock suites have been studied in various localities in the world (for example, Smith, 1931; Winchell, 1947; King, 1965; Spencer, 1969). In these suites both olivine

[1] Experimental study of the effect of total pressure on the titanium content in the pyroxene is now in progress by means of a girdle-type, high-pressure apparatus.

nephelinite and olivine melilite nephelinite are present. Spencer (1969) finds that the trend of differentiation is from olivine nephelinite to olivine melilite nephelinite. In the olivine nephelinites, olivine crystallizes first and is followed by pyroxene and nepheline. The paragenetic sequence for the olivine melilite nephelinite is olivine, pyroxene, melilite, and nepheline; perovskite occurs in some of the rocks as small crystals and appears to have crystallized late, but it also crystallized along with some of the later pyroxene, melilite, and nepheline. Perovskite also crystallized late from olivine melilite nepheline of the Honolulu series studied by Winchell (1947).

The above described natural sequence is observed in the present system and that studied by Schairer and Yoder (1964). Since melilite is always present, compositions corresponding to olivine nephelinites are not present in the system under investigation, but olivine melilitite occurs as indicated by assemblages in the diopside–akermanite–nepheline system (fig. 1). With decreasing temperature nepheline crystallizes from the liquid, producing olivine melilite nephelinite along DFMN (fig. 11). The titanium present in these olivine melilitites and olivine melilite nephelinites occurs mainly in solid solution in the clinopyroxenes. In natural rocks some of the titanium also enters the iron-titanium oxides. As the liquid descends along line DFMN, olivine, diopside$_{ss}$, nepheline$_{ss}$, and melilite continue to crystallize, the diopside incorporating more titanium in solid solution. When the maximum amount of titanium has entered the diopside$_{ss}$, perovskite begins to crystallize at reaction point (3) of figure 11. Forsterite will react with liquid at this point until consumed, the resulting assemblage along DNMP (fig. 11) becomes a melilite nephelinite. The disappearance of forsterite can also be seen in figure 2. The disappearance of forsterite by reaction is an explanation of the association of olivine-bearing and olivine-free melilite nephelinite found in nature (for example, King, 1965).

As crystallization proceeds along DMNP the liquid changes toward (4) (fig. 11), where corundum appears, and forms a six-phase assemblage. It may be possible in natural rocks that the corundum is incorporated in a spinel in the form of the hercynite molecule, a mica, or an amphibole rather than being precipitated as isolated crystals of corundum. Corundum is not present in such mafic rocks.

Natural analogues have not yet been found for the mineral assemblage shown by the reactions (1) and (2) (fig. 11). The remaining portions of the flow sheet are therefore of less petrological interest and are not considered here.

ACKNOWLEDGMENTS

Most of the present research was carried out at the University of Pittsburgh, and some parts were performed at Hokkaido University. We express our thanks to Dr. J. F. Schairer of the Geophysical Laboratory, Carnegie Institution of Washington, for his valuable suggestions during the present study; to Dr. H. S. Yoder, Jr., of the Geophysical Laboratory, to Professor H. Kuno of the University of Tokyo, and Dr.

K. Aoki of Tohoku University for critical reading of the paper; to Dr. E. G. Lidiak and Mr. A. K. Gupta of the University of Pittsburgh for performing some of the experiments and for helping to prepare the manuscript; and to Dr. A. F. Frederickson for his help in preparing experimental apparatus.

The study was financially supported by the Grant GP-5494 from the National Science Foundation, which is gratefully acknowledged.

References

Agamawi, Y. M., and White, J., 1952, The system Al_2O_3–TiO_2–SiO_2: British Ceramic Soc. Trans., v. 52, p. 293-325.

———— 1953, The quarternary system CaO–Al_2O_3–TiO_2–SiO_2, Part I. The ternary system anorthite–sphene–silica: British Ceramic Soc. Trans., v. 52, p. 271-310.

———— 1954, The quarternary system CaO–Al_2O_3–TiO_2–SiO_2, Part II. The ternary system calcium metasilicate–sphene–silica; Part III. The quarternary system calcium metasilicate–anorthite–sphene–silicate: British Ceramic Soc. Trans., v. 53, p. 1-38.

Aoki, K., 1959, Petrology of alkalic rocks of the Iki Islands and Higashi-Matsura District Japan: Tohoku Univ., Sci. Repts., 3d ser., v. 6, p. 261-310.

———— 1964, Clinopyroxenes from alkaline rocks of Japan: Am. Mineralogist, v. 49, p. 1199-1223.

———— 1967, The role of titanium in alkali basalt magmas: Japanese Assoc. Mineralogists, Petrologists, Econ. Geologists Jour., v. 57, p. 188-199.

Chayes, F., 1964, A petrographic distinction between Cenozoic volcanics in and around the open oceans: Jour. Geophys. Research, v. 69, p. 1573-1588.

Chayes, F., and Metais, D., 1964, Oceanic-island and circumoceanic basalts: Carnegie Inst. Washington Year Book 63, p. 179-182.

Deer, W. A., Howie, R. A., and Zussman, J., 1962, Rock-forming minerals, v. 1: London, Longmans, 330 p.

DeVries, R. C., Roy, Rustum, and Osborn, E. F., 1954, The system TiO_2–SiO_2: British Ceramic Soc. Trans., v. 53, p. 525-540.

———— 1955, Phase equilibria in the system CaO–TiO_2–SiO_2: Am. Ceramic Soc. Jour., v. 38, p. 158-171.

Hamilton, E. H., and Cleek, G. W., 1958, Properties of sodium titanium silicate glasses: [U.S.] Nat'l Bur. Stds. Research Jour., v. 61, p. 89-94.

Huckenholz, H. G., 1965a, Der petrogenetische Werdegand der Klinopyroxene in den tertiäen Vulkaniten der Hocheifel. I. Die Klinopyroxene der Alikali–olivin-basalt–Trachyt–Assoziation: Beitr. Mineralogie Petrographie v. 11, p. 138-195.

———— 1965b, Der Petrogenetische Werdegand der Klinopyroxene in den tertiären Vulkaniten der Hocheifel. II. Die Klinopyroxene der Basanitoide: Beitr. Mineralogie Petrographie, v. 11, p. 415-448.

———— 1966, Der petrogenetische Werdegand der Klinopyroxene in den tertiären Vukyaniten der Hocheifel. III. Die Klinopyroxene der Pikribasalte (Ankaramite): Beitr. Mineralogie Petrographie, v. 12, p. 73-95.

———— 1969, Synthesis and stability of Ti-andradite: Am. Jour. Sci., v. 267-A, Schairer v., p. 209-232.

Iwase, K., and Nisioka, U., 1936, The equilibrium diagram of the ternary system CaO–Al_2O_3·$2SiO_2$–CaO·TiO_2·SiO_2–CaO·SiO_2: Tohoku Imperial Univ. Sci. Repts., ser. 1, Honda Anniversary v., p. 444-452.

King, B. C., 1965, Petrogenesis of the alkaline igneous rock suites of the volcanic and intrusive centres of eastern Uganda: Jour. Petrology, v. 6, p. 67-100.

Kushiro, I., 1964, Petrology of the Atumi dolerite, Japan: Toyko Univ. Fac. Sci. Jour., sec. 2, v. 15, p. 135-202.

MacChesney, J. B., and Muan, A., 1960, The system iron oxide–TiO_2–SiO_2 in air: Am. Ceramic Soc. Jour., v. 43, p. 586-591.

Onuma, K., and Yagi, K., 1967, The system diopside–akermanite–nepheline: Am. Mineralogist, v. 52, p. 227-243.

Onuma, K., Hijikata, K., and Yagi, K., 1968, Unit-cell dimensions of synthetic titan-bearing clinopyroxenes: Hokkaido Univ. Fac. Sci. Jour., ser. 4, v. 14, in press.

Schairer, J. F., 1959, Phase equilibrium with particular reference to silicate systems, *in* Physicochemical measurements at high temperatures: London, Butterworths Sci. Pub., p. 117-134.

Schairer, J. F., and Bowen, N. L., 1955, The system K_2O–Al_2O_3–SiO_2: Am. Jour. Sci., v. 253, p. 681-746.

———— 1956, The system Na_2O–Al_2O_3–SiO_2: Am. Jour. Sci., v. 254, p. 129-195.

Schairer, J. F., and Yoder, H. S., Jr., 1964, Crystal and liquid trends in simplified alkali basalts: Carnegie Inst. Washington Year Book 63, p. 65-74.

Smith, H. L., and Cohen, A. J., 1963, Absorption spectra of cations in alkali-silicate glass of high ultra-violet transmission: Phys. Chem. Glasses, v. 4, p. 173-187.

Smith, W. C., 1931, A classification of some rhyolites, trachytes and phonolites from part of Kenya Coloney: Geol. Soc. London Quart. Jour., v. 72, p. 212-158.

Spencer, A. B., 1969, Alkalic igneous rocks of Uvalde County, Texas: Jour. Petrology, v. 10, in press.

Tiba, T., 1966, Petrology of the alkaline rocks of the Takakusayama district, Japan: Tohuku Univ. Sci. Rept., ser. 3, v. 9, p. 541-610.

Verhoogen, John, 1962, Distribution of titanium between silicates and oxides in igneous rocks: Am. Jour. Sci., v. 260, p. 211-220.

Winchell, H., 1947, Honolulu series, Oahu, Hawaii: Geol. Soc. America Bull., v. 58, p. 1-48.

Yagi, K., 1953, Petrochemical studies on the alkalic rocks of the Morotu district, Sakhalin: Geol. Soc. America Bull., v. 64, p. 769-810.

———— 1966, The system acmite-diopside and its bearing on the stability relations of natural pyroxenes of the acmite hedenbergite-diopside series: Am. Mineralogist, v. 51, p. 976-1000.

Yagi, K., and Onuma, K., 1967, The system $CaMgSi_2O_6$–$CaTiAl_2O_6$ and its bearing on the titanaugites: Hokkaido Univ. Fac. Sci. Jour., ser. 4, v. 13, p. 463-483.

Yoder, H. S., Jr., 1950, Stability relations of grossularite: Jour. Geology v. 58, 221-253.

Yoder, H. S., Jr., and Tilley, C. E., 1962, Origin of basaltic magma: An experimental study of natural and synthetic rock systems: Jour. Petrology, v. 3, p. 342-532.